8

Characterizing seawater constituents from optical properties

H. M. Sosik

8.1 Introduction

Most of the variability in the optical properties of the upper ocean is due to changes in the concentration and type of constituents present in the water. The optically important constituents are often of interest to ecologists and biogeochemists and include coloured dissolved organic matter, plankton and suspended sediments. Particularly in coastal waters, a wide range of dynamic processes contribute to changes in these constituents and, as a consequence, optical properties are highly variable in space and time.

In practice, understanding what drives observed optical variability is a challenging problem. Most of the constituents that contribute to optical variability are difficult to measure directly and the potential for deriving information about them from optical properties motivates much of the research in ocean optics. Optical properties can be readily measured from platforms as diverse as moorings, autonomous vehicles and earth-orbiting satellites, making them accessible at a wide range of space and time-scales. To the extent that reliable relationships between constituents and optical properties can be determined, information on constituent characteristics may be available at the same set of scales.

This chapter offers an overview of current knowledge about relationships between marine optical properties and seawater constituents. It is not an exhaustive review of this rapidly advancing topic but instead provides some historical context and an introduction to recent developments through selected examples from observational studies. Where applicable, examples have been chosen to highlight links between optical properties and phytoplankton, and harmful algal bloom (HAB) taxa, in particular.

8.2 Overview of IOP variability

Inherent optical properties (IOPs) depend only on the properties of the medium and its constituents (Preisendorfer, 1976; Kirk, 1994) and they include spectral absorption and scattering coefficients ($a(\lambda)$ and $b(\lambda)$, respectively, where λ represents wavelength) (see Table 8.1 for notation summary). The fundamental IOPs are the absorption coefficient and the volume scattering function, as various scattering coefficients (e.g. total, backward) can be determined by integration of the volume scattering function over the appropriate angles (see Morel, 2007 – Chapter 4 this volume – for more details). Measurements of the volume scattering function for natural waters are not commonly made, so this discussion is restricted to scattering coefficients.

T<small>ABLE</small> 8.1 Notation

Symbol	Definition
IOP	Inherent optical property
AOP	Apparent optical property
Chl	Chlorophyll *a* concentration, mg m^{-3}
CDOM	Chromophoric dissolved organic matter
NAP	Non-algal particles
CDM	CDOM + NAP
POC	Particulate organic carbon
PIC	Particulate inorganic carbon (calcium carbonate)
a	Absorption coefficient, m^{-1}
b	Scattering coefficient, m^{-1}
c	Beam attenuation coefficient, m^{-1}
b_b	Backscattering coefficient, m^{-1}
a_x, b_x, c_x, $b_{b,x}$	Optical coefficients where *x* is a particular seawater constituent; *x* is replaced by p, CDOM, w, ph or NAP, respectively designating particles, CDOM, water, phytoplankton and NAP
a_x^*, b_x^*	Constituent-specific optical coefficients, m^2 mg^{-1}
b_b	Backscattering ratio (b_b/b), dimensionless
λ	Wavelength, nm
z	Depth, m
S	Spectral slope for CDOM or NAP, nm^{-1}
γ	Hyperbolic spectral slope, dimensionless
$a_{<ph>}(\lambda)$	Normalized phytoplankton absorption coefficient, dimensionless
a$_x$	Absorption basis vector (spectral shape) for constituent *x*, dimensionless
b$_x$	Scattering basis vector for constituent *x*, dimensionless
A_x	Optical property amplitude for component *x*, m^{-1}
a$_{<pico>}$	Absorption basis vector for picophytoplankton, dimensionless
a$_{<micro>}$	Absorption basis vector for microphytoplankton, dimensionless
F	Dominant cell size index (amplitude), dimensionless
L_u	Upwelling radiance, W m^{-2} nm^{-1} sr^{-1}
E_d	Downwelling irradiance, W m^{-2} nm^{-1}
E_u	Upwelling irradiance, W m^{-2} nm^{-1}
$\bar{\mu}_d$	Average cosine for downwelling irradiance, dimensionless

TABLE 8.1 *(Continued)*

Symbol	Definition
$\bar{\mu}_u$	Average cosine for upwelling irradiance, dimensionless
K_d	Diffuse attenuation coefficient for downwelling irradiance, m^{-1}
K_w	Diffuse attenuation coefficient associated with water, m^{-1}
K^*_{chl}	chl - specific diffuse attenuation coefficient, $m^2\ mg^{-1}$
R_{rs}	Remote sensing reflectance, sr^{-1}
R	Irradiance reflectance, dimensionless

An important characteristic of IOPs is that they are additive. This means that, for a seawater sample containing a mixture of constituents, the absorption and scattering coefficients of the various constituents are independent, and the total coefficient can be determined by summation. This fact arises from the definition of IOPs with respect to collimated light. As discussed by Roesler and Boss (2007 – Chapter 5 this volume) current methods to measure IOPs can only approximate ideal light field and collection geometry, so corrections are sometimes required to obtain adequate estimates of true IOPs.

To explain natural variability in total IOPs and to derive estimates of ecologically and biogeochemically relevant constituents from measured IOPs, it is useful to identify categories of constituents, each of which makes a distinct contribution to the total IOPs. Typically, categories are selected on the basis of a combination of operational and functional criteria. For total $a(\lambda)$, for example, Prieur and Sathyendranath (1981) suggested partitioning into contributions from water $a_w(\lambda)$, chromophoric dissolved organic matter (CDOM) $a_{CDOM}(\lambda)$, phytoplankton $a_{ph}(\lambda)$ and non-algal particles (NAP) $a_{NAP}(\lambda)$:

$$a(\lambda) = a_w(\lambda) + a_{CDOM}(\lambda) + a_{ph}(\lambda) + a_{NAP}(\lambda). \tag{8.1}$$

Similar summations can be applied to other IOPs such as $b(\lambda)$, backscattering $b_b(\lambda)$ and the beam attenuation coefficient $c(\lambda)$, which is defined as the sum

$$c(\lambda) = a(\lambda) + b(\lambda). \tag{8.2}$$

It should be emphasized that (8.1) represents an example set of constituent categories, and the concept can be generalized to as many levels as practical or important for specific problems; in principle, different taxa of phytoplankton can be included as separate terms on the right-hand side or NAP can be separated into organic and inorganic forms, for example.

The concept of a constituent-specific optical coefficient can also be useful for understanding and predicting optical variability. A specific coefficient is one that is normalized by an index of concentration for the constituent of interest. A common example is chlorophyll-specific phytoplankton absorption:

$$a^*_{ph}(\lambda) = \frac{a_{ph}(\lambda)}{Chl}, \tag{8.3}$$

where Chl indicates the chlorophyll *a* concentration in the water. Other examples include carbon-specific scattering coefficients for phytoplankton or mass-specific scattering coefficients for mineral particles. Specific coefficients are useful because variation in the total mass of constituents is the first order source of variability in absolute IOPs. This means that, typically, specific coefficients are less variable than absolute ones, with the residual variability in specific coefficients due to differences in the characteristics of material within a particular category (e.g. changes in species composition in the phytoplankton or changes in the chemical composition or structure of mineral particles).

Linear spectral mixing is another concept that has been used to help characterize and explain IOP variability. In its simplest form, this approach can be used to represent optical contributions of two constituents, each of which has a distinct spectral shape. For example, one may consider that total particle backscattering ($b_{b,p}(\lambda)$) results from backscattering by two pools of particles, one with characteristic spectral shape $\mathbf{b_{b1}}$ and the other with shape $\mathbf{b_{b2}}$:

$$b_{b,p}(\lambda) = A_1 \mathbf{b_{b1}} + A_2 \mathbf{b_{b2}} \qquad (8.4)$$

In this expression, $\mathbf{b_{b1}}$ and $\mathbf{b_{b2}}$ represent wavelength-dependent basis vectors that describe the spectral shape of backscattering associated with particle type 1 and 2, respectively; these basis vectors are scaled to be non-dimensional. A_1 and A_2 represent the amplitudes of the scattering by particle types 1 and 2 respectively; these are scalars and thus do not vary with wavelength. If assumptions can be made concerning the relevant basis vectors and the bulk IOP is measured at multiple wavelengths, then statistical methods can be used to estimate the unknown amplitude terms in a linear mixing model such as that expressed in (8.4). The approach can be generalized to any number of terms, but unique solutions for the amplitudes depend on the spectral distinctness of the basis vectors and require at least as many spectral bands as basis vectors.

As indicated in (8.1), water molecules are important light absorbers and additionally they contribute to light scattering. Water itself is not, however, an important source of variability in IOPs in marine waters. There are some variations in spectral light attenuation by 'pure' water depending on factors such as temperature and salinity (see Pegau et al., 1997, for example), but, for the purposes of describing variations in the optical properties of the ocean, these effects are small and are not discussed further here. The following sections focus on particular water constituents and their effects on IOPs.

8.2.1   Absorption

8.2.1.1   CDOM

For optical oceanographers and many marine chemists, CDOM is operationally defined by its passage through a small pore size filter (usually 0.2 μm) and its ability to absorb visible and ultraviolet radiation. CDOM is a poorly characterized portion of the total dissolved organic matter (DOM) pool and there are no routine analytical techniques for chemically quantifying total CDOM; for this reason, CDOM is frequently quantified in terms of its measurable optical properties (i.e. absorption or fluorescence). Especially in coastal waters with substantial riverine inputs, absorption by CDOM can be very high compared with other constituents, and so it influences the quantity and colour of light penetrating into and reflecting from the upper ocean. Even in the open ocean, however, absorption by CDOM cannot be neglected (Nelson et al., 1998).

CDOM absorption is characterized by smoothly varying spectral dependence with amplitude tending to increase exponentially towards blue and ultraviolet wavelengths. For this reason its contribution to absorption is usually represented by an exponential function:

$$a_{\mathrm{CDOM}}(\lambda) = a_{\mathrm{CDOM}}(\lambda_0) e^{-S(\lambda - \lambda_0)}, \tag{8.5}$$

where λ_0 represents a reference wavelength and S is the slope of the exponential increase with decreasing wavelength (Bricaud et al., 1981). Both the amplitude and the spectral slope of a_{CDOM} depend on the composition of the dissolved organic matter pool and this in turn depends on a variety of source and sink processes. Terrestrial input, primarily from riverine sources, is significant; in addition, other processes including photooxidation (enhanced by CDOM's strong ultraviolet absorption) and local microbial activity can lead to production or loss of different forms of CDOM. These are discussed in more detail below.

CDOM fluorescence can be used as a proxy for a_{CDOM}. This topic will not be discussed further here, except to note that, as reviewed by Blough and Del Vecchio (2002), the relationship between CDOM fluorescence and absorption is complex, so regionally and temporally specific relationships must be established empirically.

8.2.1.2 *Phytoplankton*

As photosynthetic organisms, phytoplankton contain high concentrations of pigments that harvest energy from sunlight. These pigments consist of different chlorophylls and carotenoids (and, in certain taxa, biliproteins) present in varying amounts (Jeffrey and Vesk, 1997) and each type of pigment has particular spectral properties that lend phytoplankton their characteristically featured absorption spectra. Due to the ubiquitous presence of chlorophylls, absorption peaks at blue (~440 nm) and red wavelengths (~675 nm) are always present, with the blue peak broadened and enhanced by accessory pigments (Bidigare et al., 1990; see also Morel, 2007 – Chapter 4 this volume; Roesler and Boss, 2007 – Chapter 5 this volume). Pigment composition, and thus general light absorption characteristics, are partly constrained by phylogeny (Jeffrey and Vesk, 1997), but there are also important variations associated with environmental factors that affect growth (e.g. Kana et al., 1988; Sosik and Mitchell, 1991). Pigment composition and physiological status also affect the amount of light energy absorbed by phytoplankton that is reemitted as fluorescence at red wavelengths (discussed in detail in Babin, 2007 – Chapter 7 this volume).

The first order source of variation in light absorption by phytoplankton is total biomass and this, of course, depends on complex ecological and environmental factors that regulate phytoplankton growth and loss rates. Secondary effects with important consequences for how phytoplankton absorb light include variations in intracellular pigment concentration and composition and variations in cell size and shape; size and shape directly impact pigment package effects (e.g. Morel and Bricaud, 1981*a*, 1986).

8.2.1.3 *Non-algal particles*

Marine particles besides phytoplankton are also known to absorb light. In natural samples it is difficult to separate the broad category of NAP into its different contributors, which can include heterotrophic organisms such as bacteria and micrograzers, other organic particles of a detrital nature such as faecal pellets and cell debris, and

various mineral particles of both biogenic (e.g. calcite liths and shells) and terrestrial (e.g. clays and sand) origin. In comparison with phytoplankton, much less is known about the optical properties of these particles, but some generalizations have emerged.

In particular, in coastal and open ocean waters total NAP absorption tends to exhibit an absorption spectrum that monotonically increases with decreasing wavelength, similar in form to that observed for CDOM (e.g. Iturriaga and Siegel, 1989; Roesler et al., 1989; Sosik and Mitchell, 1995; Nelson et al., 1998). Consequently, a_{CDOM} can be replaced by a_{NAP} in (8.5) to provide an adequate description of NAP absorption. Despite the similar functional form found for a_{NAP} and a_{CDOM}, S values are generally not the same for these two pools, with lower values typically characteristic of particles (Roesler et al., 1989; Bricaud and Stramski, 1990; Nelson and Guarda, 1995; Bricaud et al., 1998). These observations are based on the operational definition of NAP absorption as that which is retained on a filter and not extractable by methanol following the method first proposed by Kishino et al. (1985). Because of the similar spectral character of CDOM and NAP, for some applications these pools have been combined into a single class, referred to as coloured detrital matter (CDM; which is technically a misnomer as it also includes living and inorganic matter), whose absorption follows (8.5) with a composite S parameter that will vary with the relative contributions of CDOM and NAP (Roesler et al., 1989; Siegel and Michaels, 1996; Garver and Siegel, 1997; Carder et al., 1999).

In some waters absorption by inorganic particles may also be significant, but this topic has not been well studied. Work is under way to characterize the absorption properties of specific types of mineral particles that may be important in marine systems (Babin and Stramski 2004; Stramski et al., 2004).

8.2.2 Scattering and backscattering

All particulate material whose index of refraction differs from the surrounding medium will scatter light. The amount of scattering is influenced by particle size and shape and by any absorption that occurs within the particle. In contrast to absorption, scattering is not completely characterized simply by specifying its wavelength dependence; it also has angular dependence. Total scattering is summed over all possible scattering angles, but it is also possible to define scattering coefficients over particular angular subsets. Backscattering, which is simply scattering integrated over the backward hemisphere with respect to the direction of light incidence (see Morel, 2007 – Chapter 4 this volume – for details), is a quantity that has received a lot of attention due to its importance for ocean-colour interpretation (see Section 8.4.2). As for total scattering, backscattering depends on particle concentration, size, shape and complex refractive index. Theoretical considerations show that backscattering is generally enhanced relative to forward scattering as particle size decreases, so different particles may dominate total scattering and backscattering in natural waters.

Although the dependence of light scattering on particle size, shape and refractive index is complex, some generalizations can be made on the basis of Mie theory, which applies to homogeneous, spherical particles (see e.g. Morel and Bricaud, 1986). For a given wavelength, scattering by polydisperse particles tends to increase with average particle size and with the average real part of the refractive index, so highly refractive mineral particles scatter more light than a population of bacteria of similar concentration and size distribution, for example. Furthermore, the wavelength dependence of the scattering cross-section tends to be steeper for smaller particles. Because of its

extreme small size (usually defined $<0.2\ \mu$m) and relatively dilute nature (compared with water molecules, for example), light scattering by CDOM can be neglected (see e.g. analyses by Ulloa et al., 1994; Babin et al., 2003a).

Mie theory indicates that scattering of idealized (homogeneous and spherical) non-absorbing particles varies with wavelength in a manner that depends systematically on particle size and refractive index. The wavelength dependence is often represented according to

$$b_{\mathrm{p}}(\lambda) = b_{\mathrm{p}}(\lambda_0)\left(\frac{\lambda}{\lambda_0}\right)^{-\gamma},$$

$$(8.6)$$

where λ_0 is a reference wavelength and γ represents a hyperbolic slope (Morel and Bricaud 1981b; Morel 1988). For scattering by particles that are small relative to the wavelength of light (e.g. bacteria), γ is approximately 2, whereas for larger particles γ approaches 0 (Morel and Ahn, 1990, 1991; Ahn et al., 1992). For polydisperse particles whose abundance increases with decreasing size according to a power law ('Junge' distribution), (8.6) has also been shown to hold (e.g. Boss et al., 2001a). Furthermore, (8.6) is useful for absorbing particles whose imaginary refractive index varies monotonically with wavelength (Stramski et al., 2001). If (8.6) is considered for backscattering by small monodisperse particles, γ approaches 0 (e.g. Ahn et al., 1992); whereas, Ulloa et al. (1994) have shown that, for polydisperse particles with a Junge-type size distribution, the backscattering ratio

$$\tilde{b}_{\mathrm{b,p}}(\lambda) = \frac{b_{\mathrm{b,p}}(\lambda)}{b_{\mathrm{p}}(\lambda)}$$

$$(8.7)$$

is spectrally neutral, so that $b_{\mathrm{p}}(\lambda)$ and $b_{\mathrm{b,p}}(\lambda)$ have the same γ. Non-absorbing particles and Junge-type size distributions are special cases, however, and in general $\tilde{b}_{\mathrm{b,p}}(\lambda)$ should be considered highly dependent on particle size and refractive index.

In phytoplankton cells, absorption by pigments reduces scattering preferentially at wavelengths where absorption is higher. For these and other absorbing particles, simple generalizations about spectral shape of $b_{\mathrm{p}}(\lambda)$, $b_{\mathrm{b,p}}(\lambda)$, and $\tilde{b}_{\mathrm{b,p}}(\lambda)$ cannot be made and a wide range of shapes are possible depending on the combination of particle size and complex refractive index (e.g. Bricaud et al., 1983; Bricaud and Morel, 1986; Stramski and Kiefer, 1991; Ahn et al., 1992; Stramski et al., 2001), as well as other factors such as particle shape and heterogeneity (Zaneveld and Kitchen, 1995; Gordon and Du, 2001).

For typical particle properties encountered in ocean waters, the functional form of (8.6) can reasonably be applied to $c_{\mathrm{p}}(\lambda)$, even when some of the underlying assumptions are relaxed. This has recently been discussed in detail by Boss et al. (2001a).

8.3   Relationships between IOPs and constituents

This section contains selected examples of documented relationships between IOPs and seawater constituents. Some emphasis is on studies in coastal waters, but reference to key work in open ocean waters is included as well. Not only do open ocean 'end-members' often influence coastal systems, but investigations of open ocean 'Case 1'

(Morel and Prieur, 1977) waters often set the context for characterizing more complex 'Case 2' coastal regions.

8.3.1 Chlorophyll

Since the pioneering work of Yentsch (1960, 1962), which documented that phytoplankton pigments have a significant effect on light attenuation in aquatic ecosystems, there has been a great deal of work relating optical variability to Chl. Due to its ubiquitous presence in phytoplankton and its relative ease of measurement (e.g. Yentsch and Menzel, 1963; Holm-Hansen et al., 1965), Chl is the most commonly used index of phytoplankton biomass. Especially for open ocean conditions and for absorption coefficients, relationships with Chl have been able to explain a large amount of the observed variance.

8.3.1.1 *Particle absorption*

Perhaps the most reliable optical relationships have been documented between chlorophyll and particle absorption $[a_p(\lambda) = a_{ph}(\lambda)+a_{NAP}(\lambda)]$ for Case 1 waters. Not surprisingly, this is especially true for $a_{ph}(\lambda)$, which in general is positively, although nonlinearly, correlated with Chl (Figure 8.1A). As described in Section 8.2.1, second-order variations in $a_{ph}(\lambda)$ can be examined by considering Chl-specific absorption (8.3). Notably, a variety of studies in natural waters have suggested that $a_{ph}^*(\lambda)$ values tend to be inversely related to Chl (e.g. Mitchell and Kiefer, 1988; Yentsch and Phinney, 1989; Bricaud and Stramski, 1990; Carder et al., 1991; Babin et al., 1995; Sosik and Mitchell, 1995). Bricaud et al. (1995*b*) synthesized a large data set and proposed that a power law could adequately describe this dependence across a wide range of ocean regions:

$$a_{ph}^*(\lambda) = A(\lambda)\,\text{Chl}^{B(\lambda)},\tag{8.8}$$

where parameters $A(\lambda)$ and $B(\lambda)$ are statistically determined (Figure 8.1B). There is no mechanistic basis for this particular mathematical formulation and others have been proposed (e.g. Cleveland, 1995; Lutz et al., 1996; Ciotti et al., 1999). As recently reviewed by Bricaud (2002), there is currently little consensus with respect to details of the various $a_{ph}(\lambda)$ and Chl relationships that have been published.
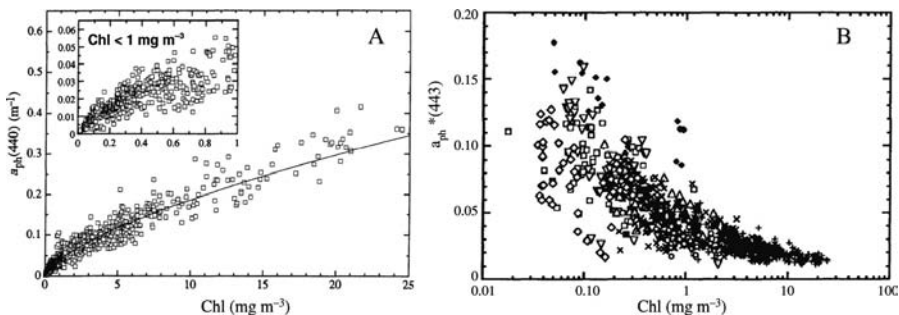

Figure 8.1
Dependence of A, $a_{ph}(440)$; B, $a_{ph}^*(44)$ on Chl for a wide range of Case 1 waters. The curve in A represents a least-squares power law fit.
Source: Bricaud et al. (1995*b*).

As mentioned in Section 8.2.2, substantial variations in $a_{ph}^*(\lambda)$ are expected due to differences in accessory pigment composition and in cell size. The applicability of relationships such as that expressed by (8.8) suggests that, in natural systems, there is a general co-variation between these cell properties and bulk Chl for example, smaller cells (with associated higher $a_{ph}^*(\lambda)$) tend to dominate in oligotrophic (i.e. low Chl) waters (see Ciotti et al., 1999 for more discussion of this topic). This is consistent with well-documented changes in planktonic community structure with trophic status (e.g. Yentsch and Phinney, 1989; Chisholm, 1992).

Despite these generalizations, it is not surprising that some variance in $a_{ph}(\lambda)$ and $a_{ph}^*(\lambda)$ cannot be explained simply by Chl. In fact, there is substantial unexplained variance in the global relationships examined by Bricaud et al. (1995b). Cleveland (1995) examined regional dependence in more detail and suggested that temperate and subtropical regions are statistically similar, but that different parameterization is required for subpolar waters. In addition, there is evidence that seasonally (Nelson and Guarda 1995) and regionally (Lutz et al., 1996; Reynolds et al., 2001) varying parameterization may be required for certain areas, and some studies of coastal areas have shown no dependence of $a_{ph}^*(\lambda)$ on Chl, within the observed dynamic range (Hoepffner and Sathyendranath, 1992). The importance of changes in accessory pigment composition (which does not necessarily covary with Chl) in explaining natural variability in $a_{ph}^*(\lambda)$ has been emphasized in several studies (e.g. Sosik and Mitchell, 1995; Allali et al., 1997). Some variations in the accessory pigment-to-chlorophyll ratios can be attributed to differences among species, while others arise from physiological responses such as photoacclimation.

In a follow-up study to their work on $a_{ph}(\lambda)$, Bricaud et al. (1998) examined patterns of variability in $a_p(\lambda)$ with respect to Chl. They reported that a similar functional form (i.e. (8.8) with $a_p^*(\lambda)$ replacing $a_{ph}^*(\lambda)$ can be useful. Their findings suggest that, for Case 1 waters, $a_{NAP}(\lambda)$ is roughly proportional to $a_p(\lambda)$, with NAP making an average contribution of 27%. Earlier observations (Bricaud and Stramski, 1990) suggested that the ratio $a_{NAP}(\lambda)/a_p(\lambda)$ might increase at lower Chl, however, more extensive studies by Cleveland (1995) and Bricaud et al. (1998) reported that, while observed variance in the ratio is high, there is no apparent trend as a function of Chl. Some observations do suggest that there are systematic deviations from the average 25–30% contribution for NAP in certain regions, including areas of the Southern Ocean (Sosik et al., 1992) and the equatorial Pacific (Bricaud et al., 1998). For Case 2 waters with significant resuspension effects or terrigenous sources of NAP, there is no expectation that $a_{NAP}(\lambda)$ will be proportional to $a_p(\lambda)$, and systematic relationships have not been described.

8.3.1.2 *Beam attenuation, scattering and backscattering*

To the extent that Chl represents an index of particle load, positive correlations may be expected with $c(\lambda)$, $b(\lambda)$ and $b_b(\lambda)$. These relationships have been explored principally because of their practical implications for Chl retrieval from satellite ocean-colour data (e.g. Gordon and Morel, 1983; Gordon et al., 1988). Early observational work summarized in Gordon and Morel (1983) suggested that, for Case 1 waters spanning a wide range of Chl, $b_p(550)$ tends to be positively correlated with Chl in a nonlinear manner that can be statistically described with a power law similar to (8.8) (but with $b_p(550)$ replacing $a_{ph}^*(\lambda)$). Voss (1992) and more recently Loisel and Morel (1998) used new observations of c_p to reevaluate this type of relationship; their

findings confirm the early generalization but also emphasize that a large amount of variance in particle scattering or attenuation cannot be explained simply on the basis of Chl (Figure 8.2). In Case 2 waters, scattering that is uncorrelated with Chl can be due to contributions of materials such as suspended sediments (e.g. Gould et al., 1999; Sosik et al., 2001), but even under Case 1 conditions, there can be important effects of non-phytoplankton scatterers such as heterotrophic organisms, particulate detritus, minerals and bubbles (e.g. Morel and Ahn, 1990; Stramski et al., 2001; Green et al., 2003*a*). Furthermore, scattering-to-chlorophyll relationships are expected to be influenced by variations in cellular carbon-to-chlorophyll (which in turn affects complex refractive index) associated with interspecific differences and photoacclimation in phytoplankton (Morel, 1987; Stramski and Morel, 1990). These effects should be evident in natural observations (e.g. Kitchen and Zaneveld, 1990; Loisel and Morel, 1998), but they cannot be unambiguously diagnosed with scattering measurements alone.

The relationship between $b_{b,p}(\lambda)$ and Chl is even more complex and a global synthesis of observations has not been put forward, though there is some evidence that Chl can explain a portion of the variability in $b_{b,p}(\lambda)$ on a regional basis (Balch et al., 2001; Reynolds et al., 2001). Models have been proposed that represent Chl dependence in such a way that $b_{b,p}(\lambda)$ amplitude increases with increasing Chl, while
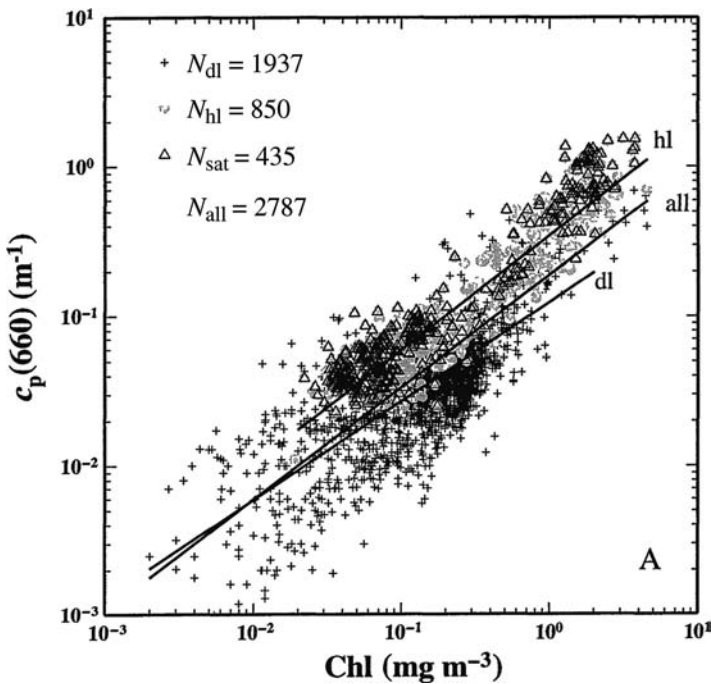

Figure 8.2
Dependence of $c_p(660)$ on Chl for a wide range of Case 1 waters. Lines indicate linear regression results, with separate lines for subsets of points from the upper layer with homogeneous Chl (hl) and from the deeper layer (dl).
Source: Loisel and Morel (1998).

the spectral slope (γ in a function of the form given by (8.6)) decreases with Chl (Gordon et al., 1988; Morel, 1988; Morel and Maritorena, 2001). Morel and Maritorena (2001) reviewed published approaches to this problem and concluded that consensus is not yet evident. Indeed, this may be an elusive goal as various lines of evidence from theoretical and observational studies suggest that, typically, phytoplankton are not an important source of $b_{b,p}(\lambda)$ variability in natural waters (Ahn et al., 1992; Stramski et al., 2001; Green et al., 2003a). Exceptions to this generalization occur in waters dominated by phytoplankton taxa with internal gas vacuoles (e.g. *Trichodesmium* sp.; Subramaniam et al., 1999) or that produce coccoliths (e.g. *Emiliania huxleyi*; Holligan et al., 1983; Balch et al., 1991). Some intriguing recent observations suggest that, during blooms of the red-tide species *Karenia brevis*, $b_{b,p}(\lambda)$ varies with Chl in a manner that differs from non-bloom conditions (Cannizzaro et al., 2007) (Figure 8.3). It is probable, however, that this reflects not the *K. brevis* cells directly, but rather some other constituent that covaries with the blooms.

Because the angular distribution of scattered light depends on the properties of the particles (i.e. size, shape and composition), indices such as the dimensionless backscattering ratio, $\tilde{b}_{b,p}$ (8.7), have also been examined with respect to dependence on Chl. While there is no simple theoretical motivation for such a relationship, one may be expected given systematic shifts in the particle composition in planktonic systems as a function of trophic status, for which Chl can be a general indicator (as discussed above, for example, in the case of observed $a_{ph}^{*}(\lambda)$ dependence on Chl). Inferences from analysis of other optical properties (e.g. Gordon et al., 1988; Morel, 1988; Morel and Maritorena, 2001) and, more recently, direct scattering observations
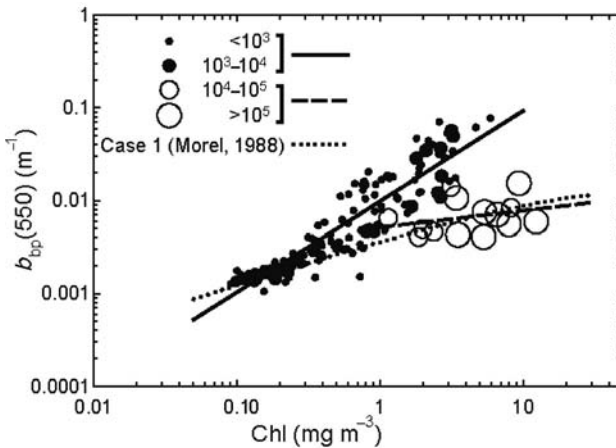

Figure 8.3
Dependence of $b_{b,p}(550)$ on Chl for the West Florida shelf during *K. brevis* bloom and non-bloom conditions. Symbols indicate ranges of observed cell concentration for *K. brevis* (cell l^{-1}) and the Case 1 water Chl-dependent $b_{b,p}(550)$ model of Morel (1988) is shown for comparison. Lines show regression results for different ranges of cell concentration and the model of Morel (1988).
Source: Cannizzaro et al. (2007).

(Twardowski et al., 2001) suggest that $\tilde{b}_{b,p}(\lambda)$ is often lower in high-chlorophyll waters (Figure 8.4). This is consistent with a trend towards more relative backscattering by large, low refractive index particles (e.g. phytoplankton cells) under eutrophic conditions. Nonetheless, variance in $\tilde{b}_{b,p}(\lambda)$ that is not explained by Chl remains high (Figure 8.4).

For scattering in general, and backscattering especially, lack of routine measurement capabilities has limited knowledge of patterns and sources of natural variability. With the recent introduction of new sensor technologies (Moore et al., 1992; Maffione and Dana, 1997; Moore et al., 2000), this situation is changing and new studies further exploring the dependence of scattering properties on water constituents are emerging (e.g. Twardowski et al., 2001; Chang et al., 2002; Babin et al., 2003a; Boss et al., 2007). This is an active area of research that is beginning to elucidate how changes in particle load and particle characteristics (i.e. size and complex refractive index) combine to determine natural light scattering properties (see below).

8.3.1.3 CDOM

Principally in an effort to simplify interpretation of remotely sensed ocean colour, there have been attempts to explain variability in the magnitude of a_{CDOM} on the basis of Chl (or a_{ph}). Some empirical results show a positive relationship (i.e. higher a_{CDOM} with higher Chl), but relationships between a_{CDOM} and Chl depend strongly on location and, as first documented by Bricaud et al. (1981), unexplained variance can be very high. In a recent example, Ciotti et al. (1999) used a linear relationship with $a_{ph}(443)$ to parameterize $a_{CDOM}(443) + a_{NAP}(443)$ in a semi-analytical model for optical properties. They found, however, that a separate 'high-CDOM' relationship was necessary for a Canadian coastal embayment, compared with coastal waters off Oregon. Moreover, for the high-CDOM case, the explained variance was very low (<10%). In a different study involving Southern Ocean waters, Reynolds et al. (2001)
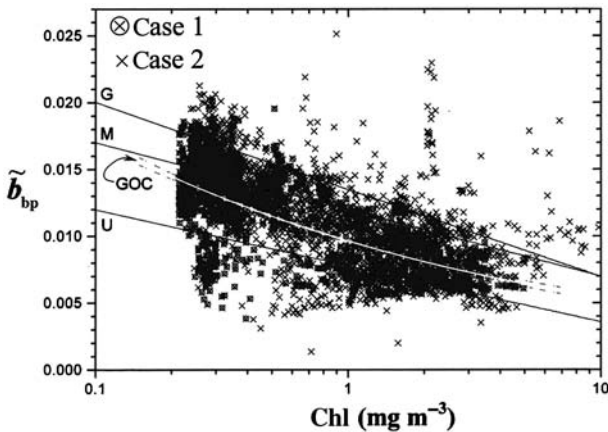

Figure 8.4
Dependence of $\tilde{b}_{b,p}$ on Chl observed in Case 1 and Case 2 waters from the Gulf of California. GOC indicates the least-squares hyperbolic fit and G, M and U show the model relationships proposed by Gordon et al. (1988), Morel (1988) and Ulloa et al. (1994), respectively.
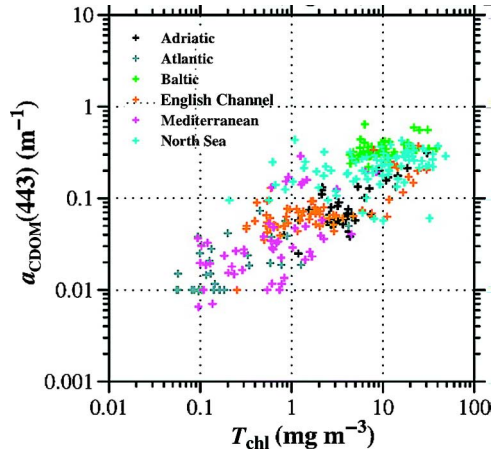*Source*: Twardowski et al. (2001).

Figure 8.5
Dependence of $a_{CDOM}(443)$ on Chl observed for a wide range of European coastal waters.
Source: Babin et al. (2003*b*).

showed that 55% of the variance in $a_{CDOM}(400)$ could be predicted from Chl with a power law (i.e. (8.8) with $a_{CDOM}(400)$ replacing $a_{ph}^{*}(\lambda)$). This approach may be least applicable for oligotrophic open ocean waters since, as reported by Nelson et al. (1998), there is no evidence of covariation between a_{CDOM} and Chl for seasonal variations in the Sargasso Sea. Probably the most complicated conditions exist over a range of coastal water types. Babin et al. (2003*b*) have emphasized this for European waters; their observations showed covariation between $a_{CDOM}(443)$ and Chl across the full dynamic range observed but also that unexplained variance can be high and that site-to-site differences are substantial (Figure 8.5). Taken together, these studies emphasize that relationships between a_{CDOM} and Chl or a_{ph} should not be assumed, and site-specific empirical verification is required before this approach can be useful.

8.3.2   CDOM and salinity

The limited capability of chlorophyll to explain variability in a_{CDOM} in many coastal locations can be understood by considering the importance of freshwater sources of CDOM. Some of the most compelling evidence for this comes from studies that document a strong correlation between a_{CDOM} and salinity. Recently, Blough and Del Vecchio (2002) reviewed knowledge about CDOM in coastal waters, including a synthesis of salinity relationships (Figure 8.6). It is apparent from these results that freshwater typically exhibits much higher values of a_{CDOM} (10 m^{-1} or greater at 355 nm) than oceanic waters (0.1 m^{-1} or less at 355 nm) and that, for many systems, first order variations in a_{CDOM} result from near-conservative mixing between freshwater and marine end members. It is also evident that the freshwater end members vary dramatically from system to system. At this time, generalizations about this variability are lacking and regional characterization is necessary to define the expected relationship between CDOM and salinity.
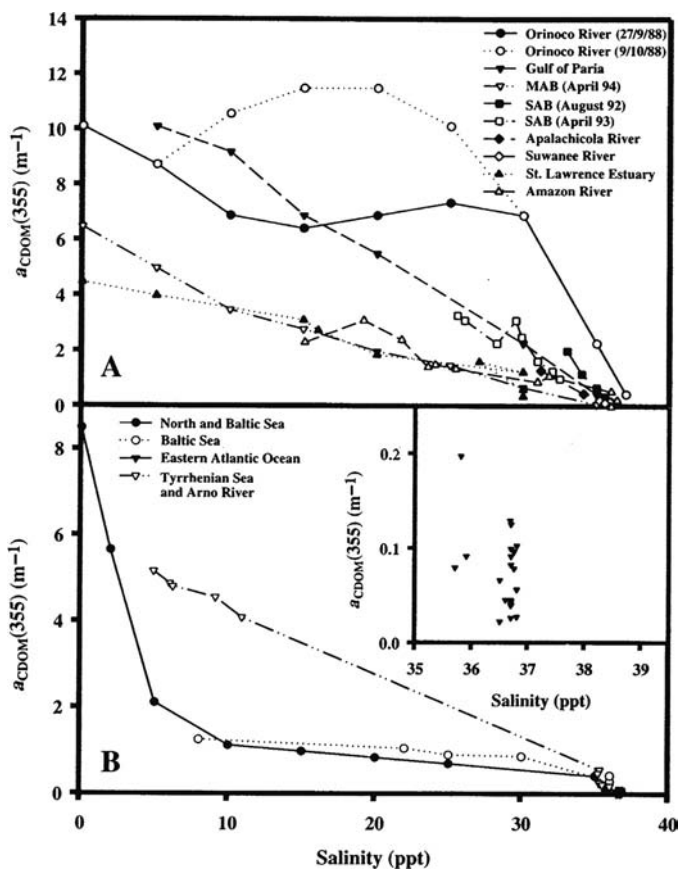
Figure 8.6.
Dependence of $a_{CDOM}(355)$ on salinity compiled from investigations of many riverine to coastal ocean systems.
Source: Blough and Del Vecchio (2002).

Relationships between a_{CDOM} and salinity are more complicated in coastal systems with mixing of more than two important water masses, as has been postulated to explain the nonlinear relationships for the North and Baltic Sea observations of Højerslev et al. (1996), for example, and the Orinoco River outflow studied by Blough et al. (1993) (Figure 8.6). Additional sources of complexity can arise from *in situ* production and loss processes. The best documented of these is photochemical oxidation, which is expected to vary seasonally in its importance. A variety of studies have shown lower a_{CDOM} for a given salinity in summer surface waters compared with other times of year and depths (e.g. Vodacek et al., 1997; Boss et al., 2001*b*), and incubation experiments have shown high rates of DOM photochemical oxidation (Kieber et al., 1990; Miller and Zepp, 1995).

Notwithstanding the strong inverse correlations between CDOM and salinity often observed over large salinity gradients, it is important to emphasize that in many locations freshwater inputs do not control CDOM variability. At salinities >~35 there is no correlation with salinity (Figure 8.6, inset). In fact, efforts to detect terrestrial
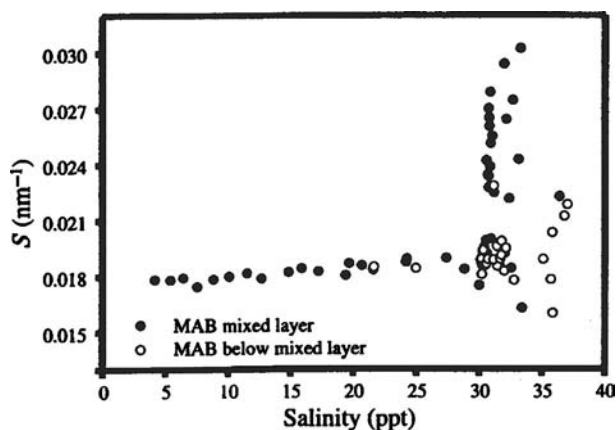
Figure 8.7
Dependence of S for a_{CDOM} on salinity observed during a transect from Delaware Bay into the continental shelf waters of the Middle Atlantic Bight. *Source*: Blough and Del Vecchio (2002).

DOM markers in the open ocean have suggested that terrestrial DOM contributes minimally in open ocean environments (Opsahl and Benner 1997). Blough and Del Vecchio (2002) point out that, given present-day annual riverine inputs and no oceanic losses, the open ocean would reach freshwater a_{CDOM} levels in ~35,000 years. The observed large a_{CDOM} gradient between freshwater and the open ocean can only be maintained if there are loss processes acting with timescales of the order of 100 years. Observations suggest that *in situ* microbial processes must be a net source of marine a_{CDOM} (Nelson et al., 1998; Twardowski and Donaghay, 2001) and that photochemical degradation of terrestrial CDOM must be significant (see review by Mopper and Kieber, 2002).

Whereas the magnitude of a_{CDOM} tends to decrease with increasing salinity, the spectral slope tends to increase (Figure 8.7). This is probably indicative of different CDOM composition. Carder et al. (1989), for example, showed that S values are higher for marine fulvic acids than for marine humic acids. Observed S values range approximately 3-fold (~0.01–0.03 nm^{-1}) with typical values of 0.015 nm^{-1} for coastal waters and 0.025 nm^{-1} for open ocean waters (Blough and Del Vecchio, 2002). There is also evidence that S values increase in response to photodegradation of CDOM (Vodacek et al., 1997; Twardowski and Donaghay, 2002). Note that care should be taken in applying (8.5) and comparing S values from different studies owing to effects of curve fitting procedure and choice of wavelength range. As detailed in Blough and Del Vecchio (2002), nonlinear curve fitting over the full ultraviolet and visible spectrum may provide the most robust and intercomparable results, while recent work by Twardowski et al. (2004) suggests that a hyberbolic model (following the form of (8.6)) may be preferable to the exponential (8.5) most commonly used to date.

8.3.3 CDOM and DOC

Dissolved organic carbon (DOC) represents an important component of the marine carbon budget and variations in its concentration are of broad interest to ecologists and geochemists. Indices of the coloured portion of DOC may be assessed from platforms

that include aircraft and earth-orbiting satellites (e.g. Vodacek et al., 1995; Siegel et al., 2002), but CDOM reflects a variable fraction of the total DOM pool and consequently relationships between CDOM properties and DOC continue to be investigated.

For coastal environments that experience freshwater influence, positive and generally linear relationships between DOC and CDOM absorption (or CDOM fluorescence) have been documented. For example, Vodacek et al. (1997) showed this for transects from Delaware Bay to the Sargasso Sea (Figure 8.8A). For river-influenced regions, these relationships typically show a high positive intercept for DOC, indicating a background level of non-coloured material. Ferrari (2000) has suggested, however, that this may not be the case for more oceanic waters (see Figure 8.8B). It is noteworthy that, in contrast to findings for coastal waters, Nelson et al. (1998) and Nelson and Siegel (2002) have shown that DOC and CDOM absorption are completely uncorrelated in the subtropical Sargasso Sea (Figure 8.8C). Even for a single coastal region, the relationship between DOC and CDOM cannot be assumed to be stable because the two can be differentially affected by source and loss processes. In the observations of Vodacek et al. (1997), for example, photodegradation of CDOM probably caused the lower CDOM levels relative to DOC in summer surface waters when compared with spring, late autumn, and also with summer samples from below the mixed layer (Figure 8.8A).

Some recent studies have suggested that CDOM absorption properties can be used to diagnose the occurrence and distribution of some different forms of CDOM containing compounds. At least two broad classes of DOM have been proposed to occur and be differentiable in marine systems: relatively refractory (slow average turnover rate) low molecular weight compounds and more labile high molecular weight compounds (e.g. Santschi et al., 1995; Guo et al., 1996). These pools are expected to have different absorption efficiency and spectral character. For coastal waters off Washington, Twardowski and Donaghay (2002) suggest that lower a_{CDOM} amplitudes and especially higher S values are characteristic under situations when there have been cumulative effects of photooxidation, and low molecular weight compounds are expected to dominate. For Equatorial Pacific waters, Simeon et al. (2003) measured two fractions of CDOM, <0.2 μm and 0.2–0.7 μm, and showed that the smaller sized material typically dominated in deep waters and exhibited higher S values compared with the larger size class in surface waters, which may be strongly influenced by biological production of labile DOM (e.g. Santschi et al., 1995).

8.3.4 SPM, POC and PIC

For most optical techniques, it is not possible to measure separately the contributions of different types of particles to the bulk signal from a water volume. For this reason many researchers have examined the relationships between optical properties, especially light scattering, and various indices of total particle load. The case of chlorophyll (discussed above) is one example, but other indices can be more appropriate depending on the environment or problem of interest. Almost without exception, these approaches have been empirical in nature with applications ranging from studies of plankton ecology to bottom boundary layer dynamics to pollution monitoring.

8.3.4.1 *Beam attenuation, scattering and backscattering*

Optically calibrated scattering coefficients are difficult to measure directly, so observations relating to particle load have typically been based on $c(\lambda)$ measurements at
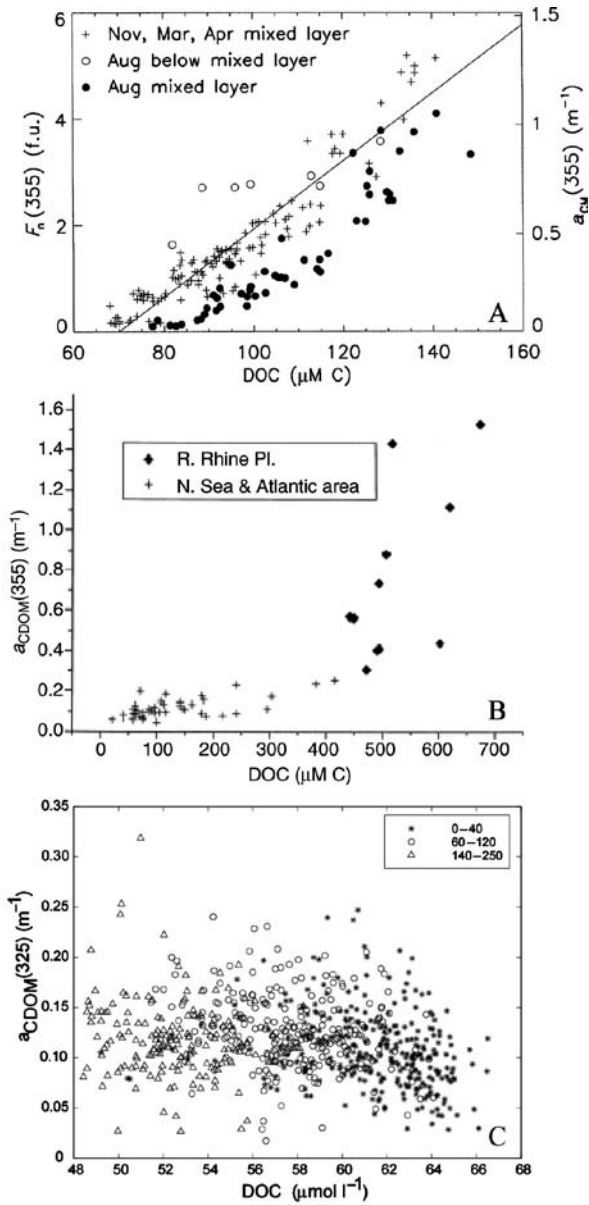
Figure 8.8
Dependence of A, CDOM fluorescence (left *y*-axis) and $a_{CDOM}(355)$ (right *y*-axis) on DOC observed during transects from Delaware Bay across the continental shelf and into the eastern Sargasso Sea;
B, $a_{CDOM}(355)$ on DOC in the Rhine River plume and other European coastal waters;
C, $a_{CDOM}(325)$ on DOC at the BATS station in the Sargasso Sea. Legend in C indicates sampling depth (m).
Sources: A, Vodacek et al. (1997); B, Ferrari (2000); C, Nelson and Siegel (2002).

wavelengths where either $a(\lambda) - a_{w}(\lambda)$ is presumed to be small or $a(\lambda) - a_{w}(\lambda)$ is also measured (such as with an ac-9 meter, see Roesler and Boss, 2007 – Chapter 5 this volume).

Total suspended particulate matter (SPM) is a common currency that is usually expressed as dry weight of particles (per unit water mass or volume) and is also referred to by different terms including seston and total suspended solids. Typically, SPM is taken to include mineral particles and plankton, as well as organic particles of detrital nature. Positive correlations between SPM and $b(\lambda)$ (or c at 660 nm) have been documented under a variety of coastal (e.g. Baker and Lavelle, 1984; Gardner et al., 2001; Babin et al., 2003a; Bergmann et al., 2004) and open ocean conditions (e.g. Gordon and Morel, 1983; Bishop, 1986; Gundersen et al., 1998) (Figure 8.9). Although scattering relationships with SPM are expected to be less variable than those with total particle volume or surface area (Carder et al., 1974), in general, SPM-specific $b_{p}(\lambda)$ (or $c(\lambda)$) coefficients,

$$b_{p}^{*}(\lambda) = \frac{b_{p}(\lambda)}{\mathrm{SPM}},$$ (8.9)

are not expected to be constant for natural particles (e.g. Baker and Lavelle, 1984). This is reflected in empirical relationships that differ among regions, because of differences in particle properties including composition and size distribution. Some systematic variations in $b_{p}^{*}(\lambda)$ have been documented; most notably, typical values are approximately twice as high in the open ocean as in coastal waters (Bishop 1986; Babin et al., 2003a). This particular finding is consistent with the conclusion that, compared with coastal waters, scattering properties of open ocean waters depend more on organic particles. Notwithstanding the general correlations that are typically found, variability in b_{p} that
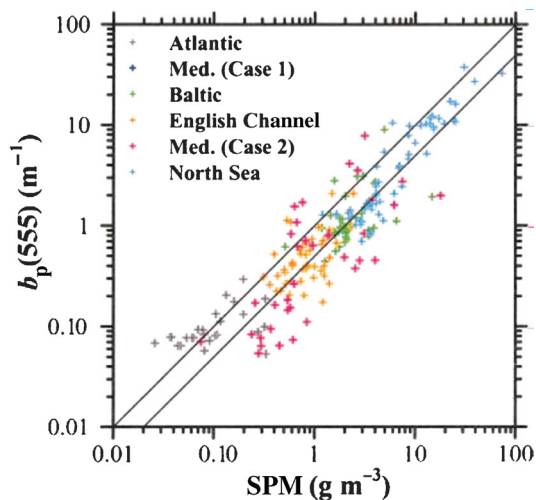

Figure 8.9
Dependence of $b_{p}(555)$ on SPM observed for a wide range of European coastal waters. Lines indicate 1:1 and 1:2.
Source: Babin et al. (2003a).

cannot be explained by SPM can be high even within local environments, and even with modern measurement and calibration techniques (e.g. Babin et al., 2003*a*) (Figure 8.9).

The heterogeneous nature of natural particle pools presents a major limitation on the generality of relationships between SPM and optical properties. There are some analytical techniques that allow subcategories of SPM to be quantified, and under certain conditions these can help to explain variability in optical properties. Particulate organic carbon (POC) concentration is one such index, which reflects contributions both from living organisms and detrital material, and its relationship with light scattering has been extensively explored, primarily for Case 1 waters. Positive linear correlations between b_p, c_p or $b_\mathrm{b,p}$ and POC have been documented for regional studies within a variety of open ocean environments (e.g. Gardner et al., 1993; Gundersen et al., 1998; Bishop, 1999; Claustre et al., 1999; Stramski et al., 1999). Within coastal waters the relative organic content of the particle pool can be highly variable and, in general, substantial variability in scattering cannot be easily related to POC (e.g. Gardner et al., 2001; Babin et al., 2003*a*) (Figure 8.10B).

Across a broad range of Case 1 conditions, the general dominance of organic particles leads to $b_\mathrm{p}(660)$ or $c_\mathrm{p}(660)$ exhibiting a near linear dependence on POC (Loisel and Morel, 1998; Bishop et al., 1999) (Figure 8.10A). In part because NAP (especially detritus) make a substantial (40–50%) contribution to c_p in these environments (DuRand and Olson, 1996; Chung et al., 1998; Claustre et al., 1999; Green et al., 2003*a*), POC is expected to explain more overall variability than chlorophyll. Even for POC within Case 1 waters, however, unexplained variability exists (Figure 8.10A), presumably associated with changes in particle properties such as size distribution and pigmentation. Within surface waters in these environments, $c_\mathrm{p}(660)$ often exhibits regular diel variations that have been used to estimate daily production or growth rates (e.g. Siegel et al., 1989; Cullen et al., 1992; DuRand and Olson, 1996; Claustre et al., 1999); these approaches are also limited by species-dependent or size-dependent variability in POC- or cell-specific scattering (e.g. DuRand and Olson, 1996).

For the special case of coccolithophore blooms, light scattering by mineral particles can dominate and particulate inorganic carbon (PIC) concentration can explain a substantial part of the variability in light scattering. This has been especially well documented in observational studies during blooms in the North Atlantic where b_p dependence on PIC can be near linear (Ackleson et al., 1994; Balch et al., 1996) (Figure 8.11). Balch et al. (2001) have recently developed an empirical approach for deriving simultaneous estimates of POC and PIC from continuous b_b observations, by alternating between measurements with and without acid pretreatment (which dissolves the particulate calcium carbonate). In addition, Guay and Bishop (2002) have developed an approach to quantify PIC on the basis of attenuation measurements with polarized light; this method should be readily adaptable for submersible applications with a modified transmissometer. Even though these new approaches may effectively separate b_p or $b_\mathrm{b,p}$ associated with calcium carbonate, absolute accuracy for optical estimates of constituent concentrations such as POC and PIC will still depend on natural variability in specific scattering properties; as mentioned above, these in turn are functions of the distributions of particle composition, size and shape. For this reason, spatially and temporally explicit empirical relationships remain essential for the highest accuracy.

In general, $b_\mathrm{b,p}(\lambda)$ is thought to depend strongly on the abundance of submicrometre detrital and mineral particles (e.g. Stramski and Kiefer, 1991; Stramski et al.,

Figure 8.10
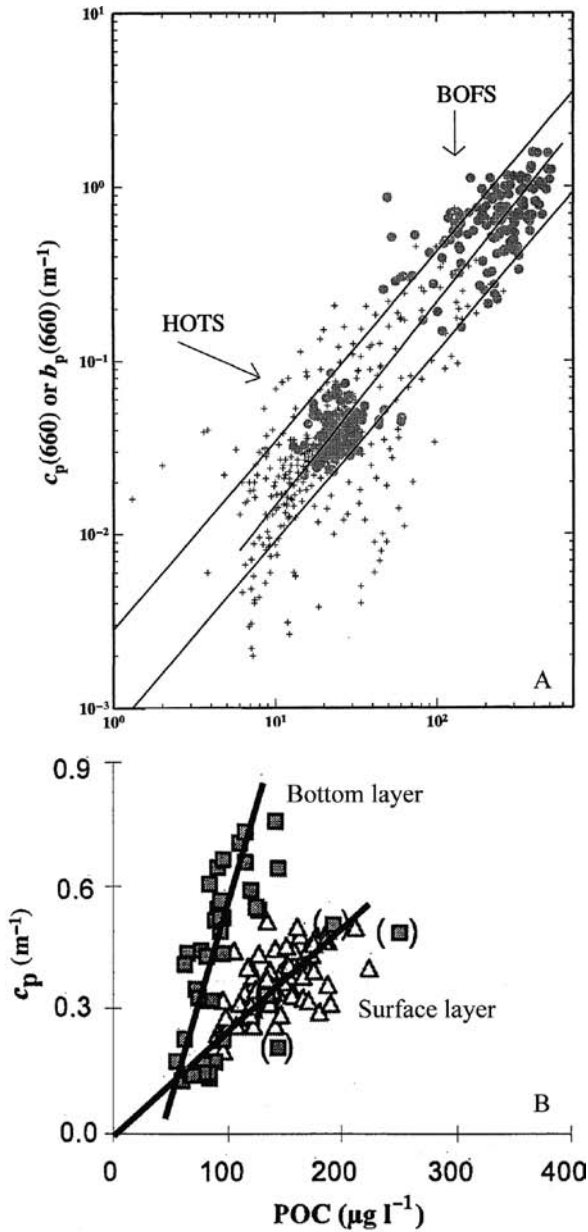Dependence of c_p(660) on POC observed for A, Case 1 waters in the
Pacific (HOTS) and Atlantic (BOFS); B, New England continental shelf
waters during stratified summer conditions. The line in B and the central
line in A are regression results, and the upper and lower lines in A bound
approximate Case 1 conditions (see Loisel and Morel, 1998, for details).
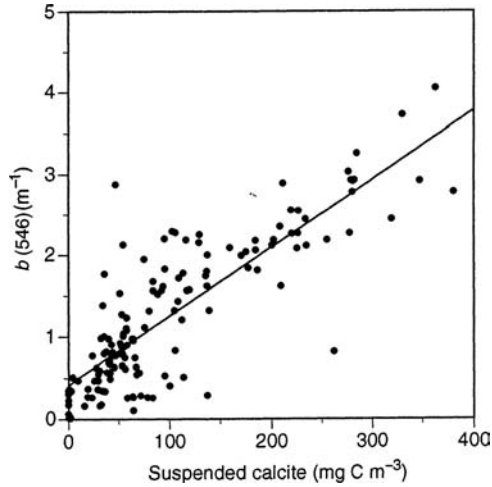*Sources*: A, Loisel and Morel (1998); B, Gardner et al. (2001).

Figure 8.11
Dependence of $b(546)$ on PIC during an *E. huxleyii* bloom in the North
Atlantic. The line represents the linear regression result.
Source: Balch et al. (1996).

2001; Green et al., 2003*a*), although observational studies of these particles and their
optical properties barely exist. Besides exceptional conditions such as coccolithophore
blooms discussed above, generalizations about $b_{b,p}(\lambda)$ dependence on particle load (or
perhaps more appropriately, indices of <1 μm particle load) are currently lacking.

8.3.4.2 Absorption

Direct relationships between absorption coefficients and indices of particle load such as
SPM and POC have not received much attention, principally because Chl is convenient
to measure and, under many circumstances, known to explain a majority of the vari-
ability in $a_p(\lambda)$. As described above (Section 8.3.1), for Case 1 waters $a_{NAP}(\lambda)$ tends to
roughly covary with $a_{ph}(\lambda)$ (Bricaud et al., 1998). In Case 2 waters, however, $a_{NAP}(\lambda)$
can be more important than $a_{ph}(\lambda)$ and the sources of NAP can be decoupled from
processes that lead to variability in Chl. For European coastal waters, $a_{NAP}(\lambda)$ has been
shown to exhibit an overall correlation with SPM, although site-specific variations in the
relationship show influences of high detrital versus high mineral loads (Bowers et al.,
1996; Babin et al., 2003*a*). More detailed interpretation of these kinds of observations is
limited by lack of knowledge of the ranges and sources of variability in specific absorp-
tion coefficients for different types of NAP, and by lack of routine analytical methods to
separate different types of NAP.

8.3.5 Particle size distribution, refractive index and pigmentation

Whereas the magnitude of absorption and scattering coefficients depend to first or-
der on the total amount of constituents in the water, other characteristics including
spectral shapes and ratios such as $\tilde{b}_{b,p}$ are more strongly influenced by the type of
constituents present. As reviewed above, light scattering and absorption properties

of particles depend on their size and complex refractive index, as well as on their shape and internal structure. The real part of the refractive index primarily governs scattering processes and is controlled by the density and composition of the particle (i.e. relative amounts of water, protein, calcite, quartz, etc.). The imaginary part governs absorption and depends strongly on the structure of pigment molecules. On the basis of theoretical understanding, combined with observational studies, some approaches have emerged that rely on distinctive optical properties to infer characteristics of the heterogeneous pool of natural particles.

8.3.5.1 Beam attenuation, scattering and backscattering

Mie theory provides a basis for understanding how different types of particles may result in distinctive spectral shapes and ratios of optical coefficients (see Bohren and Hoffman, 1983, for more details on Mie theory). Strictly, the theory applies only to homogeneous spherical particles and its forward application for a mixed assemblage of particles requires complete knowledge of the distributions of particle size and complex refractive index. Nonetheless, general inferences about the type of particles that dominate in different natural particle assemblages can be made by comparison to theoretical results (e.g. Bricaud et al., 1995a; Gould et al., 1999). Babin et al. (2003a), for example, examined the spectral shape of $b_p(\lambda)$ and $b_p(\lambda):c_p(\lambda)$ to identify Case 2 coastal European waters likely to be dominated by mineral particles and readily distinguished them from nearby Case 1 waters where phytoplankton play a dominant role (Figure 8.12). Barnard et al. (1998) examined a large spectral IOP data set from diverse environments (Cases 1 and 2) and quantified overall linear dependencies between IOPs at different wavelengths; this global result can provide a framework for comparison with local-to-regional scale spectral properties that may reflect different or site-specific patterns of constituent variability.

Figure 8.12
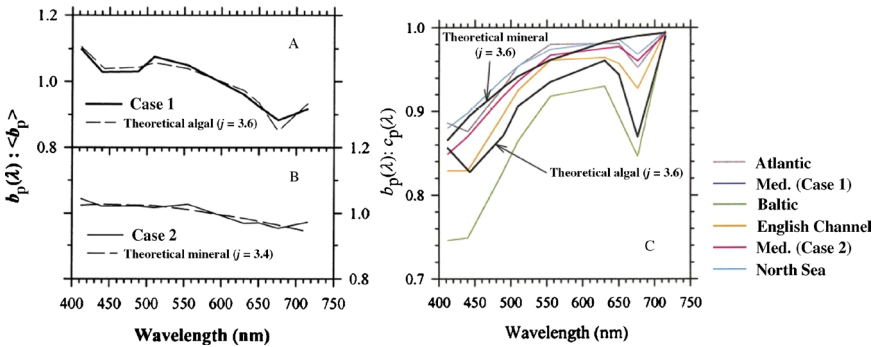Mean normalized spectral shape for $b_p(\lambda)$ observed from diverse European coastal environments with A, Case 1; B, Case 2 waters. C, mean ratios of $b_p(\lambda)$ to $c_p(\lambda)$ for each of the regions examined. For comparison, results from Mie theory are also shown for Junge-distributed (slope indicated by j values) particles with refractive indices typical for algae and minerals.
Source: Babin et al. (2003a).

There is an extensive literature on inversion methods aimed at explicitly quantifying bulk (or composite) particle properties, such as refractive index and size distribution, from light scattering (e.g. Brown and Gordon, 1974; Zaneveld et al., 1974; Kitchen et al., 1982; Bricaud et al., 1995*a*; see also review by Zaneveld et al., 2002). For example, Mie theory and observational evidence support a relatively simple relationship between the Junge slope of the particle size distribution and the spectral shape of $c(\lambda)$ (Morel, 1973; Boss et al., 2001*c*; Boss et al., 2001*a*). Twardowski et al. (2001) have built on this and developed a method that also provides bulk real refractive index estimates from IOPs that can now be measured with *in situ* sensors, that is $c(\lambda)$ and $\tilde{b}_{b,p}(532)$. Their method cannot be used to separate precisely the contributions of different types of particles in a mixture, but it can discriminate situations dominated by different broad classes of particle type. Boss et al. (2004), for example, used the approach in eastern US inner shelf waters to identify a range of bulk refractive index conditions from low values (~1.02–1.08, relative to water), indicative of phytoplankton dominance, to high values (~1.1–1.2), indicative of mineral particles (Figure 8.13). In addition to some sensitivity to violation of the assumptions of Mie theory, the approach of Twardowski et al. (2001) has other caveats, including sensitivity to lack of knowledge of particle absorption properties (imaginary refractive index) and the assumption that the particle size distribution is hyperbolic (which may be violated during near monospecific blooms, for example) (Boss et al., 2004).

Flow cytometry is one method that allows the light scattering properties of individual marine particles to be rapidly and quantitatively assessed, and thus allows distributions of properties to be observed. The method also allows differentiation of phytoplankton from NAP (e.g. Green et al., 2003*b*). Ackleson and Spinrad (1988) first showed that Mie theory-based scattering inversion methods could be applied to flow
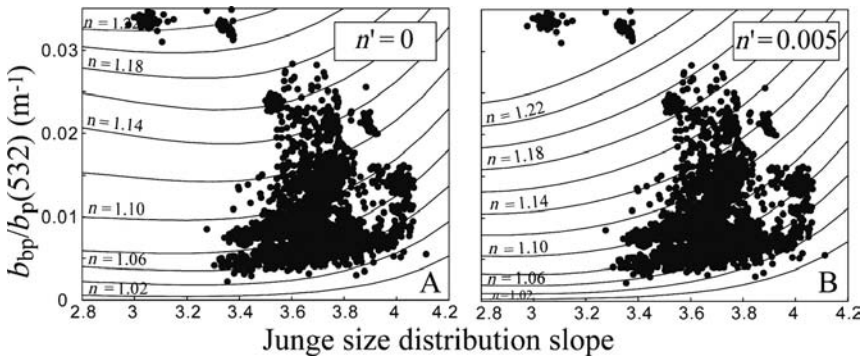
Figure 8.13

Backscattering ratio $\tilde{b}_{b,p}(532) = b_{bp}/b_p(532)$ as a function of the Junge slope of the particle size distribution. Data points correspond to *in situ* results from continental shelf waters off New Jersey, USA, with Junge slopes estimated from the spectral slope of $c(\lambda)$ (see Boss et al., 2004, for details). Variations in bulk refractive index can be constrained by comparison to contour lines, which show Mie theory for a range of real refractive indices (n) and for A, non-absorbing particles or B, absorbing particles with imaginary refractive index (n') equal to 0.005. Real refractive indices of 1.02–1.08 are characteristic of phytoplankton, whereas higher values suggest the presence of mineral particles. *Source*: Boss et al. (2004).

cytometry data for marine particles. Green et al. (2003*a*, 2003*b*; Green and Sosik, 2004) refined the approach and used it to derive particle size and refractive index distributions for different types of particles in natural samples, including various groups of microorganisms, mineral particles and detrital particles. Although flow cytometric approaches have advantages over bulk methods such as that of Twardowski et al. (2001) because detailed distributions can be explicitly derived, their application is not practical for rapid *in situ* sampling and is subject to the same limitations associated with Mie theory assumptions.

8.3.5.2   *Absorption*

In general, different chromophore and pigment molecules have different spectral absorption properties, and bulk $a_p(\lambda)$ reflects a composite spectrum of the summed contributions from all absorbing molecules present. For phytoplankton in particular, the pigments and their absorption properties are relatively well described and this has been exploited for interpretation of $a_{ph}(\lambda)$ observations from natural samples. An important category of methods for this relates to deriving information about the presence of certain taxonomic groups; these are discussed in detail in the following section. In addition to depending on phylogeny, however, pigment composition is also subject to physiological regulation and, under some circumstances, it may be possible to infer acclimation status from effects on $a_{ph}(\lambda)$. Eisner et al. (2003) have shown how this can be applied with high resolution vertical profiles in coastal waters of the north-west USA. They developed a spectral slope index for blue-to-green wavelengths of $a_p(\lambda)$ that reflected the ratio of photoprotective carotenoids to photosynthetic carotenoids in the phytoplankton (Figure 8.14). In their study over a few days, the slope index exhibited variability related to changes in stratification and incident light that is consistent with photoacclimation responses in the phytoplankton. In most cases, it will be challenging to separate these effects from those associated with changes in species composition, and this approach may not work well except at some local scales.

In addition to depending on pigment composition, the spectral shape of $a_{ph}(\lambda)$ is also sensitive to cell size. This results from pigment package effects whereby large cells and those with high internal concentrations of pigment exhibit lower absorption per pigment molecule and flatter spectra compared with smaller, less pigmented cells (e.g. Morel and Bricaud, 1981*a*, 1986). As discussed in Section 8.3.1, this effect probably contributes to the observed global trend for $a_{ph}^*(\lambda)$ to be higher in low-chlorophyll waters. Recently, Ciotti et al. (2002) have explored this idea through analysis of $a_{ph}(\lambda)$ from a range of environmental conditions. Their results showed that $a_{ph}(\lambda)$ spectral shape varied in a regular fashion with dominant cell size in natural phytoplankton assemblages, with dominant cell size able to explain 80% of the variability in spectral shape. On the basis of these findings, they developed a spectral mixing model to estimate a community level cell size index from analysis of $a_{ph}(\lambda)$ shape ($a_{<ph>}(\lambda)$, i.e. after normalization to its mean). In a manner analogous to that discussed in Section 8.2.1 for (8.4), the model represents an estimated normalized spectrum, $\hat{a}_{<ph>}(\lambda)$, as a linear sum of two basis vectors:

$$\hat{a}_{<ph>}(\lambda) = F \ \mathbf{a}_{<pico>} \ + \ (1-F)\mathbf{a}_{<micro>}, \tag{8.10}$$

where the basis vectors, $\mathbf{a}_{<pico>}$ and $\mathbf{a}_{<micro>}$, are the normalized $a_{ph}(\lambda)$ values observed for extreme cases of picophytoplankton and microphytoplankton dominated waters,
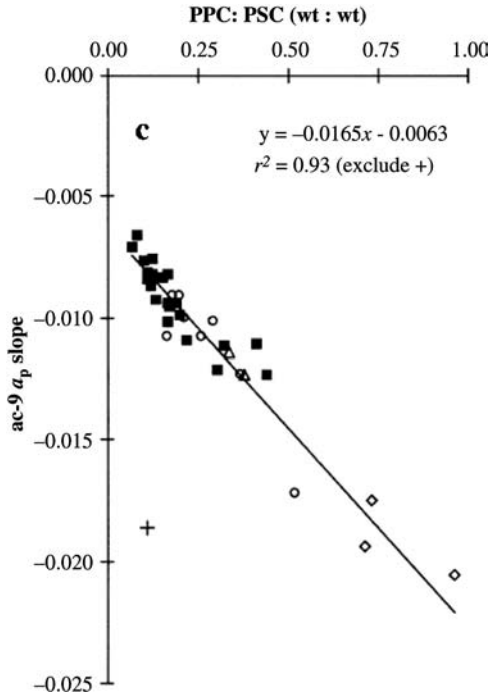
PPC: PSC (wt : wt)

$y = -0.0165x - 0.0063$
$r^2 = 0.93$ (exclude +)

c

Figure 8.14
Dependence of slope index for $a_p(\lambda)$ $(=[a_p(488) - a_p(532)]:[a_p(676)(488-532\ nm)])$ on the ratio of photoprotective carotenoids to photosynthetic carotenoids (PPC:PSC) derived from observations over several days in coastal waters of the north-west USA. The line represents the linear regression result.
Source: Eisner et al. (2003).

respectively. F ($S_{<f>}$ in the original terminology of Ciotti et al. (2002)) is a dimensionless community size index, which varies from 0 (microplankton dominated) to 1 (picoplankton dominated). The value of F for any spectrum can be selected so that it results in minimized residuals between the estimated and measured $a_{<ph>}(\lambda)$ (Figure 8.15). As pointed out by Ciotti et al. (2002), the residuals themselves can also provide information about physiological and/or taxonomic variability; for example, perhaps revealing the presence of a bloom species with distinctive pigmentation. While values of F cannot be unambiguously interpreted in terms of taxonomic composition in an assemblage, they may provide an ecologically relevant index for applications such as trophic models and estimation of biogeochemical fluxes.

8.3.6 Phytoplankton community composition

Size structure in the phytoplankton can be an informative index of community structure; however, there are many applications for which more detailed taxonomic information is desirable. Optical properties can provide some insights into taxonomic composition of a phytoplankton assemblage, but there are critical limitations for
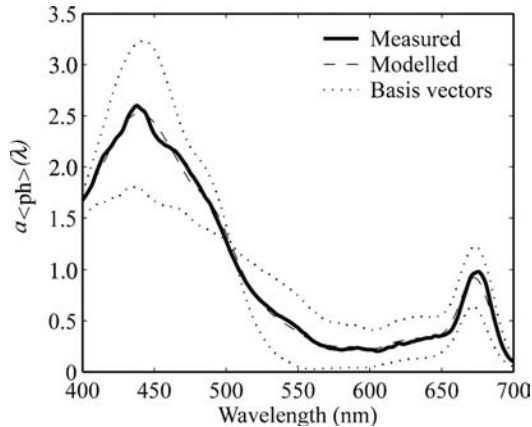
Figure 8.15
Linear spectral mixing model results estimate a phytoplankton community size index (F) from normalized $a_{ph}(\lambda)$ measured for inner shelf waters of New England during summer. The two basis vectors ('pico' and 'micro') used in the model are shown for comparison. For this example, the retrieved value of F is 0.51, indicating that the phytoplankton community is dominated by nanoplanktonic cells. See text and Ciotti et al. (2002) for model details.

all approaches, and definitive identification and enumeration at the species or genus level is not possible for many taxa without high-quality cell-imaging techniques.

Most approaches to derive information about different groups of phytoplankton from IOPs are based on absorption properties. The underlying principle is that the spectral character of absorption is strongly dependent on pigment composition, which in turn varies across taxonomic groups (Jeffrey and Vesk, 1997). Details of pigment composition derived from high-performance liquid chromatography (HPLC) can be used to characterize contributions of different algal classes to total Chl (e.g. Mackey et al., 1996). Hoepffner and Sathyendranath (1993) describe a decomposition method to estimate pigment composition from $a_{ph}(\lambda)$, allowing estimates of algal class contributions to be made without the need for more time-consuming HPLC. HPLC-based methods can only be used to discriminate classes or pigment groups (i.e. chlorophytes from diatoms from dinoflagellate, etc.), because marker pigments are generally not genus or species specific; in addition, accuracy is limited by overlap in pigment occurrence among groups and natural plasticity in pigment ratios within groups (e.g. Goericke and Montoya 1998). In addition to these caveats, spectral absorption-based approaches are further limited because some pigments that are chemically distinct have very similar absorption spectra (Bidigare et al., 1990) (i.e. diatoms may not be distinguishable from dinoflagellates despite differences in carotenoids). Indeed, distinct accessory pigment effects can be difficult to detect in natural spectra (Garver et al., 1994), and these methods require further study and careful evaluation of uncertainties.

Related spectral methods to characterize phytoplankton composition on the basis of fluorescence instead of absorption have also been proposed (e.g. Yentsch and Phinney, 1985; Beutler et al., 2002). Chlorophyll fluorescence is highly specific to phytoplankton and it reflects effects of absorption by various photosynthetic pigments,

so fluorescence excitation spectra may be decomposed to estimate the contributions of different algal groups in a mixture. Beutler et al. (2002) used a linear spectral mixing model to do this, where the basis vectors were derived from a spectral library spanning a variety of phytoplankton species. Decomposition methods for fluorescence and absorption spectra have similar limitations with respect to taxonomic specificity and accuracy (e.g. SooHoo et al., 1986), but fluorescence may have greater potential for *in situ* applications due to its sensitivity and lower interference from other constituents such as CDOM and NAP. New sensors for this kind of analysis are now becoming readily available.

Different types of absorption-based approaches rely on quantitative techniques such as derivative analysis to emphasize aspects of spectra associated with pigment composition (e.g. Millie et al., 1997) or discriminant analysis to classify spectra according to taxonomic group (e.g. Johnsen et al., 1994). The derivative approach has been most notably applied to the problem of detecting the presence of the red-tide dinoflagellate *K. brevis* in mixed assemblages. Millie et al. (1997) used the fourth derivative of absorption spectra and derived a 'similarity index' to quantify the comparison between known spectra for *K. brevis* and 'unknown' spectra for mixtures of species that may include *K. brevis*. This similarity index has been shown to be a reliable indicator for the biomass of *K. brevis* in natural samples from areas where *K. brevis* is known to bloom (Millie et al., 1997; Schofield et al., 1999; Kirkpatrick et al., 2000) (Figure 8.16). Work is under way to adapt this method to a liquid capillary waveguide application that provides high sensitivity suitable for natural cell abundances (Kirkpatrick et al., 2000). The apparent utility of this spectral approach for detection of *K. brevis* seems to be linked to the species' role as a high-light adapted organism
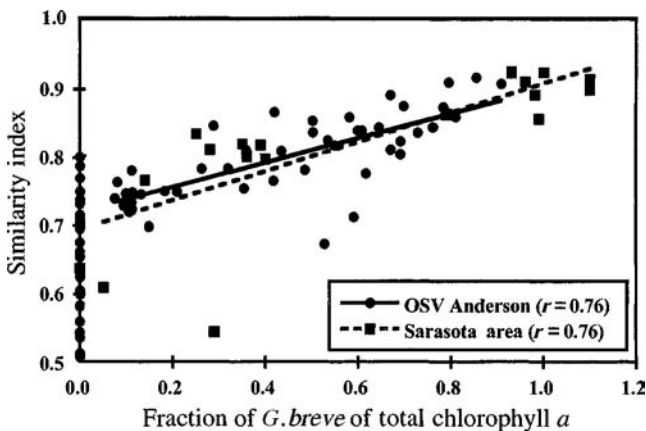
Figure 8.16
Similarity index (reflecting a comparison on fourth derivatives of normalized $a_p(\lambda)$ as described in Kirkpatrick et al. (2000)) between known *K. brevis* spectra and those for natural samples collected in the Gulf of Mexico, as it varies with the fraction of Chl attributed to *K. brevis* (previously designated *G. breve*). Lines show linear regression results for offshore (OSV Anderson) and nearshore (Sarasota) data.
Source: Kirkpatrick et al. (2000).

that forms near-monospecific blooms (Schofield et al., 1999). Recent evidence suggests that this method may have broader applicability for discriminating taxonomic groups (Millie et al., 2002).

For selected phytoplankton taxa, light scattering properties can be indicative of bloom effects. As described above (Section 8.3.1), this applies to taxa such as *Trichodesmium*, which form high concentration blooms of cells with gas vacuoles, and *E. huxleyi*, which produce high concentrations of calcium carbonate coccoliths. In practice, the presence of these blooms is most often detected through the influence of high scattering magnitude on apparent optical properties as discussed below (Section 8.5.4).

Flow cytometry is a specialized optical technique that has been used extensively to enumerate and characterize different types of phytoplankton (Olson et al., 1993; Reckermann and Colijn, 2000). This method is fundamentally different from those discussed in the rest of this chapter because it is based on light scattering and fluorescence measurements resolved for individual particles within a mixture, rather than depending on a single measurement of the bulk mixture. Despite this difference, flow cytometry is still subject to many of the same limitations with respect to the capability to discriminate taxa. It is routinely possible to enumerate separately *Prochlorococcus*, *Synechococcus,* coccolithophores, and pennate diatoms, while other groups can only be classified roughly according to cell size (e.g. Olson et al., 1989; Olson et al., 1990). With recent developments in flow cytometers, capabilities now exist for automated measurements of phytoplankton communities with submersible instruments (Dubelaar and Gerritzen, 2000; Olson et al., 2003; Sosik et al., 2003).

8.4   Overview of AOP variability

Apparent optical properties (AOPs) are determined by the IOPs and by the geometric characteristics of a natural light field (Preisendorfer, 1976; Kirk, 1994). They depend strongly enough on the IOPs that they can be characteristic of a water body and its constituents, but light field geometry must also be taken into account to completely explain their variability. AOPs are determined from measurements of radiometric quantities such as downwelling or upwelling plane irradiance, $E_d(\lambda)$ and $E_u(\lambda)$ respectively, and upwelling radiance $L_u(\lambda)$ (see Lewis, 2007 – Chapter 6 this volume – for more details). The following sections focus on how particular IOPs and seawater constituents affect AOPs.

8.4.1   Diffuse attenuation and reflectance

One of the most commonly determined AOPs is the diffuse attenuation coefficient for downwelling irradiance, $K_d(\lambda)$, which is simply the exponential rate of change in $E_d(\lambda)$ with depth z:

$$K_d(z,\lambda) = -\frac{1}{E_d(\lambda)}\frac{\mathrm{d}E_d(z,\lambda)}{\mathrm{d}z} = -\frac{\mathrm{d}\left\{\ln\left[E_d(z,\lambda)\right]\right\}}{\mathrm{d}z}. \qquad (8.11)$$

Similar diffuse attenuation coefficients can be defined for vertical profiles of any radiometric quantity – $E_u(z, \lambda)$, $L_u(z, \lambda)$, etc. The IOP dependence of $K_d(z, \lambda)$ can be considered by expressing the directionality of the light field in terms of the average cosine of the zenith angle for downwelling irradiance, $\bar{\mu}_d$, and for upwelling irradiance, $\bar{\mu}_u$, so that

$$K_{\mathrm{d}}(z,\lambda) = \frac{a(z,\lambda)+b_{\mathrm{b}}(z,\lambda)}{\bar{\mu}_{\mathrm{d}}(z)} - \frac{b_{\mathrm{b}}(z,\lambda)}{\bar{\mu}_{\mathrm{u}}(z)}R(z,\lambda),\tag{8.12}$$

where $R(\lambda)$ represents irradiance reflectance (Preisendorfer, 1961, as cited in Kirk 1994).

Spectral reflectance is another frequently measured AOP, one which is of immediate interest for ocean-colour remote sensing. Irradiance reflectance is determined according to

$$R(\lambda) = \frac{E_{\mathrm{u}}(\lambda)}{E_{\mathrm{d}}(\lambda)},\tag{8.13}$$

while 'remote-sensing' reflectance is typically defined as radiance reflectance above the sea surface:

$$R_{\mathrm{rs}}(\lambda) = \frac{L_{\mathrm{u}}(0^+,\lambda)}{E_{\mathrm{d}}(0^+,\lambda)},\tag{8.14}$$

where $L_{\mathrm{u}}(0^+,\lambda)$ and $E_{\mathrm{d}}(0^+,\lambda)$ are quantities determined just above the air-water interface ($z = 0^+$). These reflectance quantities can be viewed as depending on IOPs according to

$$R(\lambda) = f\frac{b_{\mathrm{b}}(\lambda)}{a(\lambda)+b_{\mathrm{b}}(\lambda)},\tag{8.15}$$

(shown for the example of $R(\lambda)$), where f is only approximately constant and in general varies with the angular distribution of the light field (e.g. Kirk, 1984; Morel and Gentili, 1991).

Because of their dependence on the angular distribution of the light field, AOPs for different constituents are not additive and, in the strictest sense, it is not valid to consider contributions of one constituent independent of others. Nonetheless, for some applications, $K_{\mathrm{d}}(\lambda)$ has been considered to be a 'quasi-inherent' optical property and has been approximated according to a sum of components, and constituent-specific $K_{\mathrm{d}}(\lambda)$ values have also been introduced. In a classic example where this was applied to natural water bodies, Smith and Baker (1978) proposed the relationship

$$K_{\mathrm{d}}(\lambda) = K_{\mathrm{w}}(\lambda) + \mathrm{chl}\ K_{\mathrm{chl}}^{*}(\lambda) + K_{X}(\lambda),\tag{8.16}$$

where the three terms on the right represent approximate contributions from pure seawater, from material correlated with Chl, and from other material (i.e. uncorrelated with Chl); in direct analogy with (8.3), $K_{\mathrm{chl}}^{*}(\lambda)$ is the specific coefficient for the Chl component.

8.5   AOP RELATIONSHIPS AND EXAMPLES

This section contains selected examples of documented relationships between AOPs and seawater constituents. Some emphasis is placed on quantities related to phytoplankton biomass and community composition, but other constituents are discussed where appropriate. The examples highlighted are intended to be illustrative but in no way exhaustive, considering the long history and many directions of research on these topics.

8.5.1 Chlorophyll and IOPs from irradiance

Especially in Case 1 waters, particle absorption is an important source of variability in $K_d(\lambda)$, so it is not surprising that relationships with Chl have proved robust. Morel (1988) proposed that the nonlinear dependence of $K_d(\lambda)$ on Chl could be represented by a modification to (8.16):

$$K_d(\lambda) = K_w(\lambda) + \chi(\lambda)\,\text{Chl}^{e(\lambda)}, \qquad (8.17)$$

where $\chi(\lambda)$ and $e(\lambda)$ were determined statistically for a large data set of Case 1 waters and have recently been updated (Morel and Maritorena, 2001). It is important to note that this relationship is based on a statistical analysis and does not imply that chlorophyll-containing particles are the only source of variability in $K_d(\lambda)$. Even for open ocean waters, there is strong evidence suggesting that CDM (mostly CDOM) affects seasonal patterns in $K_d(\lambda)$ (Siegel and Michaels 1996), and anomalous CDM content causes some apparent Case 1 locations to deviate from general parameterizations of (8.6) (see e.g. Morel and Maritorena, 2001, Figure 7, Mediterranean waters). To the extent that CDM effects are correlated with Chl, they are implicitly included in (8.17), but uncorrelated effects contribute to observed variance that is not explained by the equation. In coastal waters, major CDM sources, such as resuspension and riverine input, are often uncoupled from processes contributing to changes in Chl, so variability in $K_d(\lambda)$ is even more complex. Nonetheless, local-to-regional characterization of these effects can be made, and AOPs such as $K_d(\lambda)$ can be useful for long-term monitoring
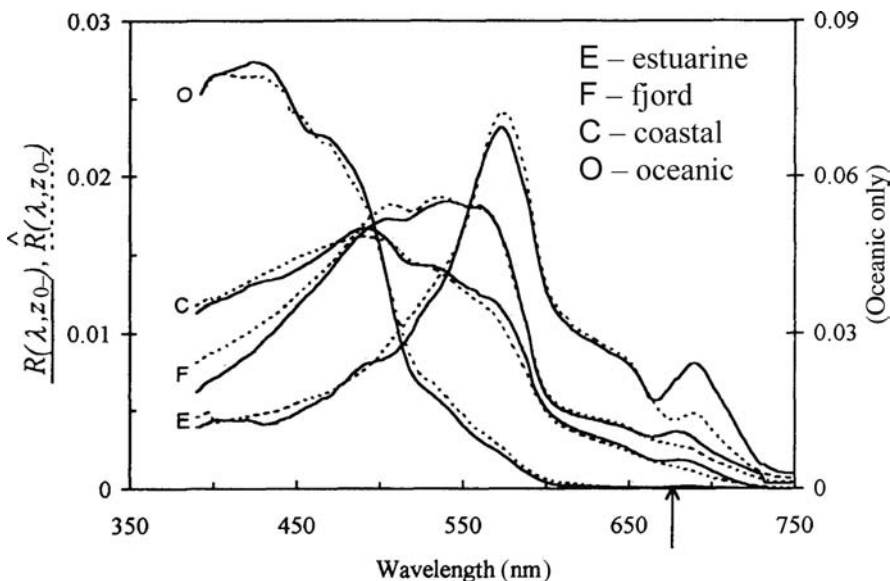

Figure 8.17
Observed (solid lines) and inversion model results (dashed lines) for reflectance spectra from a variety of water types off the north-west USA.
Source: Roesler and Perry (1995).

and early warning for blooms of algal species that contribute significantly to total Chl (Cullen et al., 1997).

Principally because widespread availability of *in situ* instrumentation for measuring IOPs is a relatively recent trend, there has been longstanding interest in analytical approaches for estimating absorption and scattering from irradiance observations (e.g. Zaneveld, 1974; Gordon et al., 1975; Kirk, 1984). These approaches remain of interest as AOPs can often be measured more easily and inexpensively than IOPs. On the basis of radiative transfer simulations, Gordon (1991), for example, proposed an inversion method to estimate $a(\lambda)$, $b(\lambda)$, and $b_b(\lambda)$ from a combination of $K_d(\lambda)$ and $R(\lambda)$ observations, given clear sky conditions and a vertically homogeneous ocean with no inelastic scattering. Subsequently, efforts have been made to reduce uncertainties in these types of inversions despite variable sky conditions, the presence of vertical stratification, variable scattering phase functions, effects of Raman scattering, and a wide range of Case 1 to Case 2 conditions (e.g. Gordon and Boynton, 1997, 1998; Loisel and Stramski, 2000; Stramska et al., 2000; Boynton and Gordon, 2002). Gordon (2002) provides an exceptional review of the history and current status of developments in this area.

By extension of the information summarized in Section 8.3, it should be possible to derive details about water constituents from IOPs that are in turn derived from AOP inversion. It is also possible to use semi-analytical approaches for direct retrieval of constituent properties from radiometric observations. Brown et al. (2004), for example, have used irradiance spectra to estimate simultaneously a_{ph} and a_{CDM} at characteristic wavelengths. A distinguishing feature of their approach is that it does not require vertical profiles, and thus can be applied to time-series irradiance observations collected from fixed-depth moored sensors or to horizontally resolved irradiance observations collected from a towed or self-propelled vehicle. As a second example, Ciotti et al. (1999) have developed a model representing diffuse attenuation coefficients and ratios of upwelling radiance in different wavebands that depends on chlorophyll and includes explicit parameterization of changes in pigment packaging, accessory pigmentation, CDOM absorption, detrital particle absorption and particle scattering. These types of approaches demonstrate the potential to derive information about constituent quantities and characteristics from AOPs. Other relevant examples are included in the following section.

8.5.2   Chlorophyll and IOPs from surface reflectance

A noteworthy subset of AOP inversion approaches relies only on surface reflectance observations; these have received a great deal of attention due to their relevance for remote sensing applications. The dependence of reflectance on IOPs, as expressed in (8.15), reveals that reflectance spectra contain information about the underlying constituents contributing to light absorption and backscattering. This has been the basis for a variety of reflectance inversion approaches developed to derive IOP or constituent estimates. The simplest are purely empirical algorithms to estimate a single constituent (e.g. Chl) from spectral ratios (e.g. Gordon et al., 1983; O'Reilly et al., 1998). More complex formulations directly use analytical expressions, such as (8.15), combined with some empirical knowledge concerning constituent IOP characteristics. In some cases, these semi-analytical inversion approaches rely on selected spectral ratios for separating constituent properties (e.g. Carder et al., 1999; Morel and Maritorena, 2001; Lee et al., 2002), while others use absolute magnitude in all available spectral

bands (e.g. Sathyendranath et al., 1989; Doerffer and Fischer, 1994; Roesler and Perry, 1995; Hoge and Lyon, 1996; Garver and Siegel, 1997; Gould et al., 2001; Reynolds et al., 2001). Furthermore, some models use a reflectance expression directly comparable with (8.15) and some assume a quadratic dependence on $\frac{b_b(\lambda)}{a(\lambda)+b_b(\lambda)}$, as proposed by Gordon et al. (1988). Semi-analytical reflectance inversion models usually provide estimates of several properties. For example, it is possible to simultaneously retrieve Chl, $a_{\mathrm{CDM}}(\lambda)$, and $b_b(\lambda)$ (e.g. Maritorena et al., 2002) (also see example in Figure 8.18).

Developments are proceeding rapidly on the topic of inverse models of surface reflectance and there is currently no consensus as to which approach is best, especially for coastal waters. In fact, it is unlikely that a single approach will work best for all applications. It is beyond the scope of this chapter to discuss and compare all existing approaches. In what follows, we focus instead on an example that typifies some general
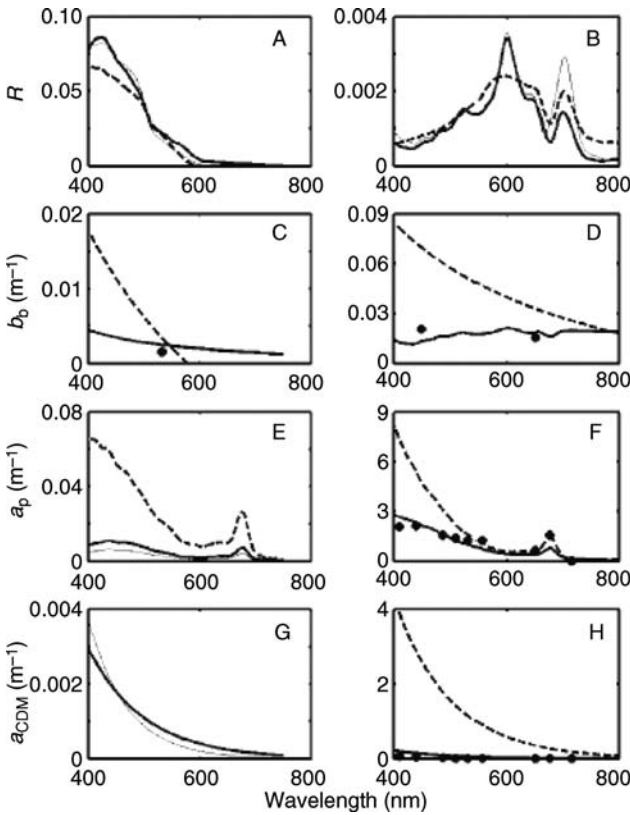

Figure 8.18
Observations (thin solid lines and symbols) and inversion results from the Roesler and Perry (1995) 'standard' model (dashed lines) and from the Roesler and Boss (2003) 'c-model' (thick solid line), for coastal waters off Oregon (left column) and off South Africa (right column).
Source: Roesler and Boss (2003).

aspects of the problem and that has also been recently applied to analysis of mixed species phytoplankton blooms.

8.5.2.1 Reflectance inversion example

The model of Roesler and Perry (1995) describes irradiance reflectance and includes effects of absorption by phytoplankton, CDOM and NAP, and backscattering by two types of particle qualitatively described as 'large' and 'small'. The basic model follows (8.15) with $a(\lambda)$ and $b(\lambda)$ determined according to linear mixing:

$$a(\lambda) = A_{\mathrm{ph1}}\mathbf{a_{ph1}} + A_{\mathrm{NAP1}}\mathbf{a_{NAP1}} + A_{\mathrm{CDOM1}}\mathbf{a_{CDOM1}} + a_{\mathrm{w}}(\lambda) \qquad (8.18)$$

and

$$b_{\mathrm{b}}(\lambda) = A_{\mathrm{bb1}}\mathbf{b_{b1}} + A_{\mathrm{bb2}}\mathbf{b_{b2}} + b_{\mathrm{b,w}}(\lambda). \qquad (8.19)$$

As in (8.4), the As here represent amplitudes for each component; and $\mathbf{a_{ph1}}$, $\mathbf{a_{NAP1}}$, $\mathbf{a_{CDOM1}}$, $\mathbf{b_{b1}}$ and $\mathbf{b_{b2}}$ represent spectral basis vectors for each type of absorber (phytoplankton, NAP, CDOM) and two types of particulate backscatters. For the model application described by Roesler and Perry (1995), $\mathbf{a_{ph1}}$ was fixed at an average shape derived from a series of direct observations in coastal waters; $\mathbf{a_{NAP1}} + \mathbf{a_{CDOM1}}$ were assumed to follow a non-dimensional form of (8.5), with a fixed S value taken from published observations; and $\mathbf{b_{b1}}$ and $\mathbf{b_{b2}}$ were set according to a non-dimensional version of (8.6) with $\gamma = 0$ and -1, respectively, to approximate backscattering contributions by pools of 'large' and 'small' (relative to the wavelength) particles. The five amplitudes $(A_{\mathrm{ph1}}, A_{\mathrm{NAP1}}, A_{\mathrm{CDOM1}}, A_{\mathrm{bb1}}, A_{\mathrm{bb2}})$ are estimated with least-squares regression to minimize the residuals between measured and modelled reflectance spectra. This approach can be used to reproduce measured reflectance spectra for a variety of waters ranging from estuarine to open ocean (Figure 8.17).

Many semi-analytical reflectance models are similar to that of Roesler and Perry (1995) and the parameterization of backscattering is an important source of error in these models. As explained in Section 8.2.3, there are well-documented deviations from the form of (8.6) for strongly absorbing particles such as phytoplankton. This may not be a problem in open ocean waters where most of the backscattering is not from phytoplankton cells, but, under bloom conditions in coastal waters, it may be critical for IOP retrieval from inverse methods. Recently, Roesler and Boss (2003) have introduced a new approach that does not require a simple constraint on the shape of the backscattering spectrum. Their model is similar to that of Roesler and Perry (1995) except that (8.6) is used for only one type of particulate backscatterer. The spectral basis vector for these particles $\mathbf{b_{b1}}$ is specified assuming that $c_{\mathrm{p}}(\lambda)$ follows a power function similar to (8.6) and that $b_{\mathrm{p}}(\lambda)$ and $b_{\mathrm{b,p}}(\lambda)$ have the same spectral shape (i.e. $\tilde{b}_{\mathrm{b,p}}$ as defined in (8.7) is independent of wavelength). This leads to

$$\mathbf{b_{b1}} = \frac{A_{\mathrm{cp1}}\mathbf{c_{p1}} - A_{\mathrm{ph1}}\mathbf{a_{ph1}} - A_{\mathrm{NAP1}}\mathbf{a_{NAP1}}}{A_{\mathrm{b1}}}, \qquad (8.20)$$

which is a non-dimensional form of $c_p(\lambda) - a_p(\lambda)$. In Roesler and Boss (2003), the basis vectors $\mathbf{a}_{ph1}$ and $\mathbf{a}_{NAP1}$ were specified as in Roesler and Perry (1995) and the basis vector for beam attenuation was taken as

$$\mathbf{c}_{p1} = \left(\frac{\lambda}{\lambda_0} \right)^{-\gamma}. \tag{8.21}$$

This latter assumption is based on the observations that variations in the functional form of the spectral dependence for $c_p(\lambda)$ are more restricted than for $b_{b,p}(\lambda)$, and that spectral variations in $\tilde{b}_{b,p}$ are weak. An interesting feature of this model is that inversion for IOPs produces not only the more standard $a(\lambda)$ and $b_b(\lambda)$ retrievals, but also $c(\lambda)$ estimates.

Roesler and Boss (2003) applied this 'c-model' to invert measured $R(\lambda)$ for IOPs, with γ and five amplitude terms derived by least-squares minimization. They also compared results to those for the standard Roesler and Perry (1995) model in which the basis vectors for particle backscattering are taken to follow simple power laws, that is as in (8.6). From this analysis, it was evident that both models can reproduce the major features of measured $R(\lambda)$ for different water types, although the c-model performed better for fine details (Figures 8.18A, 8.18B). The c-model markedly outperformed the standard model in IOP retrieval (Figures 8.18C to 8.18H). Because inversion of the c-model provides estimates of $c(\lambda)$ amplitude and spectral slope (γ), there is potential for obtaining information about the shape of the particle size distribution (see Section 8.3.5 and Boss et al., 2001a, for example). Further assessment of this and related models, especially comparison of retrieval results with independent measurements for a variety of water types, is currently needed.

8.5.3   Empirical algorithms for SPM, POC and PIC

Besides those for retrieving Chl (discussed in Sections 8.5.1 and 8.5.2), empirical algorithms relating SPM to AOPs have been most widely pursued. As reviewed by Kirk (1994), there have been a number of efforts to derive total SPM from remotely sensed reflectance, most developed for local or regional application in coastal or inland waters. Some approaches are based on reflectance intensity at red or near-infrared wavelengths, whereas others depend on changes in spectral shape, and applications have been developed for satellite-based sensors including Landsat, AVHRR, CZCS, SeaWiFS and others. In general, differences in particle size and composition can be extreme and, because this leads to large variations in mass-specific scattering, a universal empirical algorithm for SPM is unlikely to emerge.

Some recent efforts have focused on the potential for particular subcategories of SPM to be retrieved from remotely sensed reflectance. Stramski et al. (1999) used empirical relationships between $R(555)$ and $b_b(510)$ and between POC and $b_{b,p}(510)$ for Southern Ocean waters to derive seasonal POC maps from SeaWiFS observations. This approach has been further developed for application in the Mediterranean (Loisel et al., 2001) and another related empirical approach (on the basis of a correlation between POC and SeaWiFS-derived normalized water-leaving radiance at 555 nm) has been proposed for the South Atlantic (Mishonov et al., 2003). Loisel et al. (2002) have used satellite-based observations to examine global patterns of seasonality in $b_{b,p}(490)$ and to estimate the global surface POC pool. While these methods may yield acceptable results for many oceanic conditions, their accuracy will undoubtedly be compromised

under certain situations common in coastal waters, including those with high loads of mineral particles. In fact, even within two regions of the Southern Ocean, Stramski et al. (1999) observed significant differences in the relationship between POC and $b_{b,p}(510)$.

A second subcategory of SPM that is amenable to remote sensing is PIC, specifically particulate calcite present in coccoliths produced during *E. huxleyi* or other coccolithophore blooms. Semi-analytical models can be formulated to include the effects of calcite-specific scattering (Gordon et al., 1988; Ackleson et al., 1994; Tyrell et al., 1999; Smyth et al., 2002), although multiple constituent retrievals can be a problem in these applications. Gordon et al. (2001) developed an approach to map PIC on the basis of red and near-infrared SeaWiFS bands, combined with an experimentally determined relationship between $b_b(\lambda)$ and coccolith calcite concentration. This approach has the advantage of being relatively independent of effects of Chl and CDOM absorption. Regardless of the algorithm form, retrieval of PIC depends on knowledge of calcite-specific backscattering (Balch et al., 1991; Balch et al., 1996; Voss et al., 1998) and natural variability within and between species may ultimately constrain accuracy (Balch et al., 1999).

8.5.4 Phytoplankton community composition

The possibility that information about the taxonomic composition of phytoplankton may be retrieved from analysis of AOPs, especially reflectance, is attractive to plankton ecologists. If robust techniques for this can be developed, then spatially and temporally resolved maps of community structure may be derived from satellites, vertical moorings and other platforms.

In a strict sense, this goal remains elusive, and for the same reasons as for IOPs there is no theoretical or empirical evidence to suggest that it can ever be achieved with the rigour of other more conventional methods for quantitatively describing community structure, such as microscopy and molecular genetic analyses. Nevertheless, there are several well-documented circumstances under which AOPs can be used to provide information about occurrence and distribution of particular bloom taxa.

8.5.4.1 *Empirical algorithms for particular taxa*

The most successful efforts to quantify the occurrence of particular types of phytoplankton from AOPs have been based on empirical analysis of surface reflectance properties. Blooms of taxa associated with distinctive light-scattering properties, such as the coccolithophore *E. huxleyi* and the filamentous cyanobacterium *Trichodesmium* sp., can be detected in satellite imagery. *E. huxleyi* blooms and their associated highly scattering coccoliths produce milky white patches visible from space (e.g. Holligan et al., 1983) and empirical classification algorithms that are based on spectral water-leaving radiance have been used to map global bloom distribution (Brown and Yoder 1994; Iglesias-Rodríguez et al., 2002). *Trichodesmium* blooms also produce distinctive highly reflective, discoloured patches that have been identified empirically in ocean color images (Subramaniam and Carpenter, 1994; Subramaniam et al., 2002). For the purpose of detecting both *E. huxleyi* and *Trichodesmium*, efforts to develop analytical models for remote sensing reflectance have begun to be explored (Ackleson et al., 1994; Subramaniam et al., 1999; Tyrell et al., 1999). Local- or region-specific approaches may also be effective for discriminating waters dominated by different

taxonomic groups; for example, as shown by Bergmann et al. (2004) for diatom-versus cryptophyte-dominated communities in Lake Michigan. For taxa of special interest, such as the red-tide dinoflagellate *K. brevis* common on the west Florida coast, remote sensing algorithms have been used to monitor possible blooms in the context of historical knowledge about bloom seasonality and distribution (Stumpf, 2001). For the case of *K. brevis* off Florida, further work to develop a more explicit taxon-specific approach is also being pursued since these blooms have been shown to have different chlorophyll-specific scattering from other waters in the region (e.g. Cannizzaro et al., 2004).

Most efforts to detect particular taxa on the basis of AOPs rely on distinctive scattering characteristics; however, absorption properties may also be useful for some cases. Kahru and Mitchell (1998) have exploited characteristic absorption features at ultraviolet (UV) wavelengths to identify red-tide blooms from $R_{rs}(\lambda)$ observations extending into the UV. They showed that these bloom species off southern California exhibit enhanced UV absorption (at 380 nm; associated with micosporine-like amino acids) compared with background conditions, and this can be readily detected in reflectance band ratios. Currently, this kind of approach cannot be implemented for satellite imagery because the sensors lack UV bands, but future ocean-colour missions may include such a capability. Another possibility is that effects of the characteristic absorption peaks associated with phycobiliproteins in cyanobacteria may be detectable in AOPs (Sathyendranath et al., 1994), although this may only be practical under extreme bloom conditions (Morel, 1997).

8.5.4.2 *Reflectance inversion to retrieve multiple taxa*

Especially for application to phytoplankton blooms composed of multiple taxa, an important limitation of the reflectance inversion approaches discussed in Section 8.5.2 is that they typically assume a single fixed spectral basis vector for $a_{ph}(\lambda)$. As the shape of $a_{ph}(\lambda)$ is known to vary with factors such as pigment content and cell size, this simplification may lead to errors in retrieved constituent IOPs. To address this problem in the case of some specific bloom waters, Roesler et al. (2003) introduced a replacement for the first term in (8.18) that accounts for five separate basis vectors:

$$a_{ph}(\lambda) = \sum_{i=1}^{5} A_{phi}\mathbf{a_{phi}}, \qquad (8.22)$$

where, as above, the amplitudes, A_{phi}, are estimated and the basis vectors, $\mathbf{a_{phi}}$, are specified *a priori*, in this case, for each phytoplankton type i. For application to red-tide bloom waters off South Africa, Roesler et al. (2004) determined $\mathbf{a_{phi}}$ from a combination of microscopic and spectrophotometric analysis of various particle size fractions from discrete water samples. They then inverted $R(\lambda)$ measurements to estimate the separate contributions of diatoms, dinoflagellates (except *Dinophysis*), *Dinophysis*, *Mesodinium* and chlorophytes during evolution of a red-tide bloom (Figure 8.19). This is a compelling demonstration of the possibility to retrieve taxonomic information about phytoplankton community structure from remote sensing measurements; however, it is important to recognize that this goal was possible because the basis vectors for $a_{ph}(\lambda)$ were carefully determined from water samples collected during the bloom. Moreover, the example comes from bloom conditions under which phytoplankton dominated both the IOPs and AOPs. Further research is required to determine how broadly this promising approach can be applied.
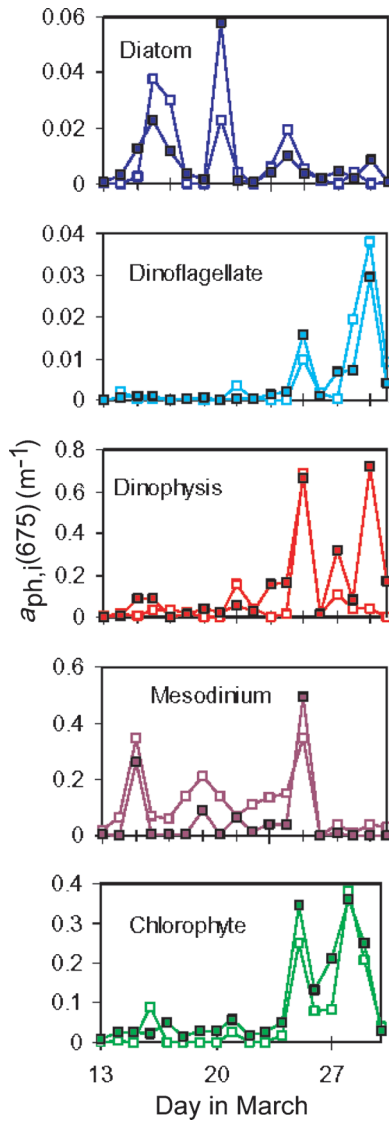
Figure 8.19
Contributions of different phytoplankton groups to total $a_{ph}(675)$ during a bloom sequence in South African coastal waters estimated from microscopic observations (open symbols) and from the reflectance inversion model (solid symbols) of Roesler et al. (2004). See text for details.
Source: Roesler et al. (2004).

8.6 Optical properties and HABs – summary comments

In assessing the relationships between HABs and optical properties, it is critical to consider that spatial, temporal and ecological characteristics of HABs vary dramatically and in ways that have optical implications. For example, some taxa form near monospecific blooms of such an extent that they dominate the phytoplankton biomass over large space and timescales. In some other cases, such as the one presented in Section 8.5.4, mixed species blooms can be responsible for total biomass that is so high that the absorption and scattering associated with phytoplankton exceeds that for other particulate and dissolved material. In these cases, bulk IOPs and AOPs have great potential to provide information about bloom dynamics, and a wide range of measurement approaches from microscale IOP meters (Roesler and Boss, 2007 – Chapter 5 this volume) to regional scale remote sensing of surface AOPs (Ruddick et al., 2007 – Chapter 9 this volume) are useful. Even in these cases, however, extracting information about specific bloom taxa from bulk optical properties remains a research topic.

Another extreme are spatially and temporally localized HABs where a single species increases in abundance, yet remains a small portion of the total phytoplankton biomass. In some cases these blooms can even be localized to thin (meter-scale or less) subsurface vertical layers. These are generally not amenable to detection by satellite or airborne remote sensing. Direct optically based detection of these HAB species *in situ* requires specialized techniques under development such as cell-level imaging or optical indicators linked with molecular probing (see e.g. Scholin et al., 2007 – Chapter 11 this volume). For these types of HAB, more conventional optical approaches may be most appropriate for general characterization of the environmental conditions under which the HAB phenomena occur.

Cullen (2007 – Chapter 1 this volume) proposes a classification system for HABs that is based on environmental and ecological characteristics, some of which have a direct bearing on optical consequences. This kind of assessment should be a first step in identifying which of the optical techniques and measurement approaches reviewed here may be effective components of an ocean observing system for HAB monitoring and research. Depending on the HAB problem of interest, the goals for an observing system may span from environmental characterization to species-specific detection to prediction of bloom transport and fate (Schofield et al., 2007 – Chapter 3 this volume). It cannot be overstated that no one approach or set of approaches can be recommended for all types of HABs. Informed choices must be made about sampling strategy, including which properties to target and the appropriate space and timescales for observation. The knowledge summarized here about advantages and limitations of various optical approaches for providing information on seawater constituents should be an important consideration in making these decisions.

8.7 Conclusion – opportunities and challenges

The optical properties of seawater depend on so many characteristics of the water's constituents that the problem of their interpretation presents at once great opportunities and great challenges. If the relationships between optical properties and constituent properties were very simple, then the potential for insights would be well constrained but relatively limited. In fact, the complexity of factors contributing to optical

variability currently limits the accuracy with which we can extract information about ecological and biogeochemical properties from optical observations. At the same time, the potential to derive new and more accurate information continues to be alluring.

The present state of this field is strengthened by several lines of theoretical underpinning and by observational generalizations that have emerged over years of inquiry. These foundations provide a ready frame of reference for investigating exceptions and intriguing results that continue to defy easy interpretation, such as the optical properties of near-monospecific phytoplankton blooms. Developments in this area are proceeding rapidly and we can continue to look forward to new and fundamental insights.

Potential ecological applications for optical observations span a great range of space and timescales, as well as requiring various degrees of accuracy and specificity. This means that general conclusions about current status and future needs and potential are difficult to make. For many of the examples presented in this chapter, there are well documented relationships between optical properties and constituents that are evident when the full range of observed variability (a 'global' data set) is considered. When these relationships are examined in closer detail, however, it is common to find that the global generalization does not apply at many smaller scales. At the same time, there are a variety of cases where local (in space or time) relationships between optical properties and constituent properties can be well defined and understood. These can be exploited for many important applications, but not indiscriminately extrapolated to larger or different scales.

In the end, the choice of relevant optical properties and interpretation approaches must depend on the problem of interest. In many cases, difficulties or limitations with interpretation are more than offset by the sampling advantages. Almost without exception, ecologists do not have tools or methods for sampling quantities of interest in the ocean over the scales and with the resolution that important questions require. Optical properties that are practical to measure at timescales ranging from microseconds to years and on space scales from micrometres to thousands of kilometres have great appeal. A model that will probably continue to be productive is that of local-to-regional scale optical sampling, combined with periodic or intermittent (perhaps guided) discrete sampling for detailed analysis of constituents or properties of interest.

References

ACKLESON, S. G., BALCH, W. M. and HOLLIGAN, P. M. 1994. The response of water-leaving radiance to particulate calcite and pigment concentration: a model for Gulf of Maine coccolithophore blooms. *J. Geophys. Res.*, 99, pp. 7483–500.

ACKLESON, S. G. and SPINRAD, R. W. 1988. Size and refractive index of individual marine particulates: a flow cytometric approach. *Appl. Opt.*, 27, pp. 1270–77.

AHN, Y. H., BRICAUD, A. and MOREL, A. 1992. Light backscattering efficiency and related properties of some phytoplankters. *Deep Sea Res.*, 39, pp. 1835–55.

ALLALI, K., BRICAUD, A. and CLAUSTRE, H. 1997. Spatial variations in the chlorophyll-specific absorption coefficients of phytoplankton and photosynthetically active pigments in the equatorial Pacific. *J. Geophys. Res.*, 102, pp. 12413–23.

BABIN, M. 2007. Phytoplankton fluorescence: theory, current literature and *in situ* measurement. In: Babin et al. (eds), op. cit., this volume.

BABIN, M., MOREL, A., FOURNIER-SICRE, V., FELL, F. and STRAMSKI, D. 2003a. Light scattering properties of marine particles in coastal and open ocean waters as related to the particle mass concentration. *Limnol. Oceanogr.*, 48, pp. 843–59.

Babin, M., Roesler, C. S. and Cullen, J. J. (eds). 2007. *Real-time Coastal Observing Systems for Marine Ecosystem Dynamics and Harmful Algal Blooms: Theory, Instrumentation and Modelling*. Paris, Intergovernmental Oceanographic Commission of UNESCO. (Monographs on Oceanographic Methodology.)

Babin, M., Stramski, D., Ferrari, G. M., Claustre, H., Bricaud, A., Obolensky, G. and Hoepffner, N. 2003*b*. Variations in the light absorption coefficients of phytoplankton, nonalgal particles, and dissolved organic matter in coastal waters around Europe. *J. Geophys. Res.*, 108, 3211, doi:3210.1029/2001JC000882.

Babin, M. and Stramski, D. 2004. Variations in the mass-specific absorption coefficient of mineral particles suspended in water. *Limnol. Oceanogr.*, 49, pp. 756–67.

Babin, M., Therriault, J. C., Legendre, L., Nieke, B., Reuter, R. and Condal, A. 1995. Relationship between the maximum quantum yield of carbon fixation and the minimum quantum yield of chlorophyll *a in vivo* fluorescence in the Gulf of St. Lawrence. *Limnol. Oceanogr.*, 40, pp. 956–68.

Baker, E. T. and Lavelle, J. W. 1984. The effect of particle size on the light attenuation coefficient of natural suspensions. *J. Geophys. Res.*, 89, pp. 8197–203.

Balch, W. M., Drapeau, D. T., Cucci, T. L., Vaillancourt, R. D., Kilpatrick, K. A. and Fritz, J. J. 1999. Optical backscattering by calcifying algae: separating the contribution of particulate inorganic and organic carbon fractions. *J. Geophys. Res.*, 104, pp. 1541–58.

Balch, W. M., Drapeau, D. T., Fritz, J. J., Bowler, B. C. and Nolan, J. 2001. Optical backscattering in the Arabian Sea – continuous underway measurements of particulate inorganic and organic carbon. *Deep Sea Res. I*, 48, pp. 2423–52.

Balch, W. M., Holligan, P. M., Ackleson, S. G. and Voss, K. J. 1991. Biological and optical properties of mesoscale coccolithophore blooms in the Gulf of Maine. *Limnol. Oceanogr.*, 36, pp. 629–43.

Balch, W. M., Kirkpatrick, K. A., Holligan, P., Harbour, D. and Fernandez, E. 1996. The 1991 coccolithophore bloom in the central North Atlantic. 2: Relating optics to coccolith concentration. *Limnol. Oceanogr.*, 41, pp. 1684–96.

Barnard, A. H., Pegau, W. S. and Zaneveld, J. R. V. 1998. Global relationships of the inherent optical properties of the oceans. *J. Geophys. Res.*, 103, pp. 24955–68.

Bergmann, T., Fahnenstiel, G., Lohrenz, S., Millie, D. and Schofield, O. 2004. The impacts of recurrent resuspension events and variable phytoplankton community composition on remote sensing reflectance. *J. Geophys. Res.*, 109, C10S15, doi:10.1029/2002JC001575.

Beutler, M., Wiltshire, K. H., Meyer, B., Moldaenke, C., Lüring, C., Meyerhöfer, M., Hansen, U. P. and Dau, H. 2002. A fluorometric method for the differentiation of algal populations *in vivo* and *in situ*. *Photosyn. Res.*, 72, pp. 39–53.

Bidigare, R. R., Ondrusek, M. E., Morrow, J. H. and Kiefer, D. 1990. *In vivo* absorption properties of algal pigments. *Ocean Optics X, Proc. SPIE*, 1302, pp. 290–302.

Bishop, J. K. B. 1986. The correction and suspended matter calibration of Sea Tech transmissometer data. *Deep Sea Res.*, 33, pp. 121–34.

Bishop, J. K. B. 1999. Transmissometer measurement of POC. *Deep Sea Res. I*, 46, pp. 353–69.

Bishop, J. K. B., Calvert, S. E. and Soon, M. Y. S. 1999. Spatial and temporal variability of POC in the northeast Subarctic Pacific. *Deep Sea Res. II*, 46, pp. 2699–733.

Blough, N. V. and Del Vecchio, R. 2002. Chromophoric DOM in the coastal environment. In: D. A. Hansell and C. A. Carlson (eds), *Biogeochemistry of Marine Dissolved Organic Matter*. New York, Academic Press, pp. 509–46.

Blough, N. V., Zafiriou, O. C. and Bonilla, J. 1993. Optical absorption spectra of waters from the Orinoco River outflow: terrrestrial input of colored organic matter to the Caribbean. *J. Geophys. Res.*, 98, pp. 2271–78.

Bohren, C. F. and Hoffman, D. R. 1983. *Absorption and Scattering of Light by Small Particles*. New York, John Wiley & Sons.

Boss, E., Pegau, W. S., Gardner, W. D., Zaneveld, J. R. V., Barnard, A. H., Twardowski, M. S., Chang, G. C. and Dickey, T. D. 2001*c*. Spectral particulate attenuation and particle

size distribution in the bottom boundary layer of a continental shelf. *J. Geophys. Res.*, 106, pp. 9509–16.

Boss, E., Pegau, W. S., Lee, M., Twardowski, M., Shybanov, E., Korotaev, G. and Baratange, F. 2004. Particulate backscattering ratio at LEO 15 and its use to study particle composition and distribution. *J. Geophys. Res.*, 109(C1), doi:10.1029/2002JC001415.

Boss, E., Pegau, W. S., Zaneveld, J. R. V. and Barnard, A. H. 2001*b*. Spatial and temporal variability of absorption by dissolved material at a continental shelf. *J. Geophys. Res.*, 106, pp. 9499–507.

Boss, E., Twardowski, M. S. and Herring, S. 2001*a*. Shape of the particulate beam attenuation spectrum and its inversion to obtain the shape of the particulate size distribution. *Appl. Opt.*, 40, pp. 4885–93.

Bowers, D. G., Harker, G. E. L. and Stephan, B. 1996. Absorption spectra of inorganic particles in the Irish Sea and their relevance to remote sensing of chlorophyll. *Int. J. Rem. Sens.*, 17, pp. 2449–60.

Boynton, G. C. and Gordon, H. R. 2002. Irradiance inversion algorithm for absorption and backscattering profiles in natural waters: Improvements for clear waters. *Appl. Opt.*, 41, pp. 2224–27.

Bricaud, A. 2002. Inherent optical properties of particles in Case 1 waters: The various parameterizations and their consistency. *Ocean Optics XVI, Proc.* pp. 1–8.

Bricaud, A., Babin, M., Morel, A. and Claustre, H. 1995*b*. Variability in the chlorophyll-specific absorption coefficients of natural phytoplankton: Analysis and parameterization. *J. Geophys. Res.*, 100, pp. 13321–32.

Bricaud, A. and Morel, A. 1986. Light attenuation and scattering by phytoplankton cells: a theoretical modeling. *Appl. Opt.*, 25, pp. 571–80.

Bricaud, A., Morel, A., Babin, M., Allali, K. and Claustre, H. 1998. Variations of light absorption by suspended particles with chlorophyll *a* concentration in oceanic (Case 1) waters: analysis and implications for bio-optical models. *J. Geophys. Res.*, 103, pp. 31033–44.

Bricaud, A., Morel, A. and Prieur, L. 1981. Absorption by dissolved organic matter of the sea (yellow substance) in the UV and visible domains. *Limnol. Oceanogr.*, 26, pp. 43–53.

Bricaud, A., Morel, A. and Prieur, L. 1983. Optical efficiency factors of some phytoplankters. *Limnol. Oceanogr.*, 28, pp. 816–32.

Bricaud, A., Roesler, C. and Zaneveld, J. R. V. 1995*a*. *In situ* methods for measuring the inherent optical properties of ocean waters. *Limnol. Oceanogr.*, 40, pp. 393–410.

Bricaud, A. and Stramski, D. 1990. Spectral absorption coefficients of living phytoplankton and non-algal biogenous matter: a comparison between the Peru upwelling area and the Sargasso Sea. *Limnol. Oceanogr.*, 35, pp. 562–82.

Brown, C. A., Huot, Y., Purcell, M. J., Cullen, J. J. and Lewis, M. R. 2004. Mapping coastal optical and biogeochemical variability using an Autonomous Underwater Vehicle (AUV) and a new bio-optical inversion algorithm. *Limnol. Oceanogr. Meth.*, 2, pp. 262–81.

Brown, C. W. and Yoder, J. A. 1994. Coccolithophorid blooms in the global ocean. *J. Geophys. Res.*, 99, pp. 7467–82.

Brown, O. B. and Gordon, H. R. 1974. Size-refractive index distribution of clear coastal water particulates from light scattering. *Appl. Opt.*, 13, pp. 2874–81.

Cannizzaro, J. P., Carder, K. L., Chen, R. F., Heil, C. A. and Vargo, G. A. 2007. A novel technique for detection of the toxic dinoflagellate, *Karenia brevis*, in the Gulf of Mexico from remotely sensed ocean color data. *Cont. Shelf Res.*

Carder, K. L., Betzer, P. R. and Eggimann, D. W. 1974. Physical, chemical, and optical measures of suspended-particle concentrations: their intercomparison and application to the West African Shelf. In: R. J. Gibbs (ed.), *Suspended Solids in Water*. New York, Plenum Press, pp. 173–93.

Carder, K. L., Chen, F. R., Lee, Z. P. and Hawes, S. K. 1999. Semianalytic moderate-resolution imaging spectrometer algorithms for chlorophyll *a* and absorption with bio-optical domains based on nitrate-depletion temperatures. *J. Geophys. Res.*, 104, pp. 5403–21.

CARDER, K. L., HAWES, S. K., BAKER, K. A., SMITH, R. C., STEWARD, R. G. and MITCHELL, B. G. 1991. Reflectance model for quantifying chlorophyll *a* in the presence of productivity degradation products. *J. Geophys. Res.*, 96, pp. 20599–611.

CARDER, K. L., STEWARD, R. G., HARVEY, G. R. and ORTNER, P. B. 1989. Marine humic and fulvic acids: their effects on remote sensing of ocean chlorophyll. *Limnol. Oceanogr.*, 34, pp. 68–81.

CHANG, G. C., DICKEY, T. D., SCHOFIELD, O. M., WEIDEMANN, A. D., BOSS, E., PEGAU, W. S., MOLINE, M. A. and GLENN, S. M. 2002. Nearshore physical processes and bio-optical properties in the New York Bight. *J. Geophys. Res.*, 107, 3133, doi:3110.1029/2001JC001018.

CHISHOLM, S. W. 1992. Phytoplankton size. In: P. G. Falkowski and A. D. Woodhead (eds), *Primary Productivity and Biogeochemical Cycles in the Sea*. New York, Plenum Press, pp. 213–37.

CHUNG, S. P., GARDNER, W. D., LANDRY, M. R., RICHARDSON, M. J. and WALSH, I. D. 1998. Beam attenuation by microorganisms and detrital particles in the equatorial Pacific. *J. Geophys. Res.*, 103, pp. 12669–81.

CIOTTI, A. M., CULLEN, J. J. and LEWIS, M. R. 1999. A semi-analytical model of the influence of phytoplankton community structure on the relationship between light attenuation and ocean color. *J. Geophys. Res.*, 104, pp. 1559–78.

CIOTTI, A. M., LEWIS, M. R. and CULLEN, J. J. 2002. Assessment of the relationships between dominant cell size in natural phytoplankton communities and the spectral shape of the absorption coefficient. *Limnol. Oceanogr.*, 47, pp. 404–17.

CLAUSTRE, H., MOREL, A., BABIN, M., CAILLIAU, C., MARIE, D., MARTY, J. C., TAILLIEZ, D. and VAULOT, D. 1999. Variability in particle attenuation and chlorophyll fluorescence in the tropical Pacific: scales, patterns, and biogeochemical implications. *J. Geophys. Res.*, 104, pp. 3401–22.

CLEVELAND, J. S. 1995. Regional models for phytoplankton absorption as a function of chlorophyll *a* concentration. *J. Geophys. Res.*, 100, pp. 13333–44.

CULLEN, J. J. 2007. Observation and prediction of harmful algal blooms. In: Babin et al. (eds), op. cit., this volume.

CULLEN, J. J., CIOTTI, A. M., DAVIS, R. F. and LEWIS, M. R. 1997. Optical detection and assessment of algal blooms. *Limnol. Oceanogr.*, 42, pp. 1223–39.

CULLEN, J. J., LEWIS, M. R., DAVIS, C. O. and BARBER, R. T. 1992. Photosynthetic characteristics and estimated growth rates indicate grazing is the proximate control of primary production in the equatorial Pacific. *J. Geophys. Res.*, 97, pp. 639–54.

DOERFFER, R. and FISCHER, J. 1994. Concentrations of chlorophyll, suspended matter, and gelbstoff in Case II waters derived from satellite coastal zone color scatter data with inverse modeling methods. *J. Geophys. Res.*, 99, pp. 6457–7466.

DUBELAAR, G. B. J. and GERRITZEN, P. L. 2000. CytoBuoy: a step forward towards using flow cytometry in operational oceanography. *Scientia Marina*, 64, pp. 255–65.

DURAND, M. D. and OLSON, R. J. 1996. Contributions of phytoplankton light scattering and cell concentration changes to diel variations in beam attenuation in the equatorial Pacific from flow cytometric measurements of pico-, ultra- and nanoplankton. *Deep Sea Res. I*, 43, pp. 891–906.

EISNER, L. B., TWARDOWSKI, M. S., COWLES, T. J. and PERRY, M. J. 2003. Resolving phytoplankton photoprotective: photosynthetic carotenoid ratios on fine scales using *in situ* spectral absorption measurements. *Limnol. Oceanogr.*, 48, pp. 632–46.

FERRARI, G. M. 2000. The relationship between chromophoric dissolved organic matter and dissolved organic carbon in the European Atlantic coastal area and in the West Mediterranean Sea (Gulf of Lions). *Mar. Chem.*, 70, pp. 339–57.

GARDNER, W. D., BLAKEY, J. C., WALSH, I. D., RICHARDSON, M. J., PEGAU, S., ZANEVELD, J. R. V., ROESLER, C., GREGG, M. C., MACKINNON, J. A., SOSIK, H. M. and WILLIAMS, A. J. 3RD. 2001. Optics, particles, stratification, and storms on the New England continental shelf. *J. Geophys. Res.*, 106, pp. 9473–97.

GARDNER, W. D., WALSH, I. D. and RICHARDSON, M. J. 1993. Biophysical forcing of particle production and distribution during a spring bloom in the North Atlantic. *Deep Sea Res. II*, 40, pp. 171–95.

GARVER, S. and SIEGEL, D. 1997. Inherent optical property inversion of ocean color spectra and its biogeochemical interpretation. 1: Time series from the Sargasso Sea. *J. Geophys. Res.*, 102, pp. 18607–25.

GARVER, S. A., SIEGEL, D. A. and MITCHELL, B. G. 1994. Statistical variability of near-surface particulate absorption spectra: what can a satellite ocean color imager see? *Limnol. Oceanogr.*, 39, pp. 1349–67.

GOERICKE, R. and MONTOYA, J. P. 1998. Estimating the contribution of microalgal taxa to chlorophyll *a* in the field-variations of pigment ratios under nutrient- and light-limited growth. *Mar. Ecol. Progr. Ser.*, 169, pp. 87–95.

GORDON, H. R. 1991. Absorption and scattering estimates from irradiance measurements: Monte Carlo simulations. *Limnol. Oceanogr.*, 36, pp. 769–77.

GORDON, H. R. 2002. Inverse methods in hydrologic optics. *Oceanologia*, 44, pp. 9–58.

GORDON, H. R. and BOYNTON, G. C. 1997. Radiance irradiance inversion algorithms for estimating the absorption and backscattering coefficients of natural waters: homogeneous waters. *Appl. Opt.*, 36, pp. 2636–41.

GORDON, H. R. and BOYNTON, G. C. 1998. Radiance irradiance inversion algorithm for estimating the absorption and backscattering coefficients of natural waters: vertically stratified water bodies. *Appl. Opt.*, 37, pp. 3886–96.

GORDON, H. R., BOYNTON, G. C., BALCH, W. M., GROOM, S. B., HARBOUR, D. S. and SMYTH, T. J. 2001. Retrieval of coccolithophore calcite concentration from SeaWiFS imagery. *Geophys. Res. Lett.*, 28, pp. 1587–90.

GORDON, H. R., BROWN, O. B., EVANS, R. H., BROWN, J. W., SMITH, R. C., BAKER, K. S. and CLARK, D. K. 1988. A semianalytic radiance model of ocean color. *J. Geophys. Res.*, 93, pp. 10909–24.

GORDON, H. R., BROWN, O. B., and JACOBS, M. M. 1975. Computed relationships between the inherent and apparent optical properties of a flat homogeneous ocean. *Appl. Opt.*, 14, pp. 417–27.

GORDON, H. R., CLARK, D. K., BROWN, J. W., BROWN, O. B., EVANS, R. H. and BROENKOW, W. W. 1983. Phytoplankton pigment concentrations in the Middle Atlantic Bight: comparison of ship determinations and CZCS estimates. *Appl. Opt.*, 22, pp. 20–36.

GORDON, H. R. and DU, T. 2001. Light scattering by nonspherical particles: application to coccoliths detached from *Emiliana huxleyi*. *Limnol. Oceanogr.*, 46, pp. 1438–54.

GORDON, H. R. and MOREL, A. 1983. *Remote Assessment of Ocean Color for Interpretation of Satellite Visible Imagery. A Review*. New York, Springer-Verlag.

GOULD, R. W. JR, ARNONE, R. A. and MARTINOLICH, P. M. 1999. Spectral dependence of the scattering coefficient in Case 1 and Case 2 waters. *Appl. Opt.*, 38, pp. 2377–83.

GOULD, R. W. JR, ARNONE, R. A. and SYDOR, M. 2001. Absorption, scattering, and remote-sensing reflectance relationships in coastal waters: testing a new inversion algorithm. *J. Coast. Res.*, 17, pp. 328–41.

GREEN, R. E. and SOSIK, H. M. 2004. Analysis of apparent optical properties and ocean color models using measurements of seawater constitutents in New England continental shelf surface waters. *J. Geophys. Res.*, 109, C03026, doi:03010.01029/02003JC001977.

GREEN, R. E., SOSIK, H. M. and OLSON, R. J. 2003*a*. Contributions of phytoplankton and other particles to inherent optical properties in New England continental shelf waters. *Limnol. Oceanogr.*, 48, pp. 2377–91.

GREEN, R. E., SOSIK, H. M., OLSON, R. J. and DURAND, M. D. 2003*b*. Flow cytometric determination of size and complex refractive index for marine particles: comparison with independent and bulk estimates. *Appl. Opt.*, 42, pp. 526–41.

GUAY, C. K. H. and BISHOP, J. K. B. 2002. A rapid birefringence method for measuring suspended CaCO$_3$ concentrations in seawater. *Deep Sea Res. I*, 49, pp. 197–210.

GUNDERSEN, J. S., GARDNER, W. D., RICHARDSON, M. J. and WALSH, I. D. 1998. Effects of monsoons on the seasonal and spatial distributions of POC and chlorophyll in the Arabian Sea. *Deep Sea Res. II*, 45, pp. 2103–32.

GUO, L., SANTSCHI, P. H., CIFUENTES, L. A., TRUMBORE, S. E. and SOUTHON, J. 1996. Cycling of high-molecular-weight dissolved organic matter in the Middle Atlantic Bight as revealed by carbon isotopic (^{13}C and ^{14}C) signatures. *Limnol. Oceanogr.*, 41, pp. 1242–52.

HOEPFFNER, N. and SATHYENDRANATH, S. 1992. Bio-optical characteristics of coastal waters: absorption spectra of phytoplankton and pigment distribution in the western North Atlantic. *Limnol. Oceanogr.*, 37, pp. 1660–79.

HOEPFFNER, N. and SATHYENDRANATH, S. 1993. Determination of the major groups of phytoplankton pigments from the absorption spectra of total particulate matter. *J. Geophys. Res.*, 98, pp. 22789–803.

HOGE, F. E. and LYON, P. E. 1996. Satellite retrieval of inherent optical properties by linear matrix inversion of oceanic radiance models: an analysis of model and radiance measurement errors. *J. Geophys. Res.*, 101, pp. 16631–48.

HØJERSLEV, N. K., HOLT, N. and AARUP, T. 1996. Optical measurements in the North Sea-Baltic Sea transition zone. I. On the origin of the deep water in the Kattegat. *Cont. Shelf Res.*, 16, pp. 1329–42.

HOLLIGAN, P. M., VIOLLIER, M., HARBOUR, D. S., CAMUS, P. and CHAMPAGNE-PHILIPPE, M. 1983. Satellite and ship studies of coccolithophore production along a continental shelf edge. *Nature*, 304, pp. 339–42.

HOLM-HANSEN, O., LORENZEN, C. J., HOLMES, R. W. and STRICKLAND, J. D. H. 1965. Fluorometric determination of chlorophyll. *J. Cons. Int. Explor. Mer*, 30, pp. 3–15.

IGLESIAS-RODRÍGUEZ, M. D., BROWN, C. W., DONEY, S. C., KLEYPAS, J., KOLBER, D., KOLBER, Z., HAYES, P. K. and FALKOWSKI, P. G. 2002. Representing key phytoplankton functional groups in ocean carbon cycle models: Coccolithophorids. *Global Biogeochem. Cy.*, 16, 1100, doi: 1110.1029/2001GB001454.

ITURRIAGA, R. and SIEGEL, D. A. 1989. Microphotometric characterization of phytoplankton and detrital absorption properties in the Sargasso Sea. *Limnol. Oceanogr.*, 34, pp. 1706–26.

JEFFREY, S. W. and VESK, M. 1997. Introduction to marine phytoplankton and their pigment signatures. In: S. W. Jeffrey, R. F. C. Mantoura and S. W. Wright, (eds), *Phytoplankton Pigments in Oceanography: Guidelines to Modern Methods*. Paris, UNESCO, pp. 37–84.

JOHNSEN, G., SAMSET, O., GRANSKOG, L. and SAKSHAUG, E. 1994. *In vivo* absorption characteristics in 10 classes of bloom-forming phytoplankton: taxonomic characteristics and responses to photoadaptation by means of discriminant and HPLC analysis. *Mar. Ecol. Progr. Ser.*, 105, pp. 149–57.

KAHRU, M. AND MITCHELL, B. G. 1998. Spectral reflectance and absorption of a massive red tide off southern California. *J. Geophys. Res.*, 103, pp. 21601–09.

KANA, T. M., GLIBERT, P. M., GOERICKE, R. and WELSCHMEYER, N. A. 1988. Zeaxanthin and β-carotene in *Synechoccus* WH7803 respond differently to irradiance. *Limnol. Oceanogr.*, 33, pp. 1623–27.

KIEBER, R. J., ZHOU, X. and MOPPER, K. 1990. Formation of carbonyl compounds from UV-induced photodegradation of humic substances in natural waters: fate of riverine carbon in the sea. *Limnol. Oceanogr.*, 35, pp. 1503–15.

KIRK, J. T. O. 1984. Dependence of relationship between inherent and apparent optical properties of water on solar altitude. *Limnol. Oceanogr.*, 29, pp. 350–56.

KIRK, J. T. O. 1994. *Light and Photosynthesis in Aquatic Ecosystems*. Cambridge, UK, Cambridge University Press.

KIRKPATRICK, G. J., MILLIE, D. F., MOLINE, M. A. and SCHOFIELD, O. 2000. Optical discrimination of a phytoplankton species in natural mixed populations. *Limnol. Oceanogr.*, 45, pp. 467–71.

KISHINO, M., TAKAHASHI, N., OKAMI, N. and ICHIMURA, S. 1985. Estimation of the spectral absorption coefficients of phytoplankton in the sea. *Bull. Mar. Sci.*, 37, pp. 634–42.

KITCHEN, J. C. and ZANEVELD, J. R. V. 1990. On the non-correlation of the vertical structure of light scattering and chlorophyll *a* in Case I waters. *J. Geophys. Res.*, 95, pp. 20237–46.

KITCHEN, J. C., ZANEVELD, J. R. V. and PAK, H. 1982. Effect of particle size distribution and chlorophyll content on beam attenuation spectra. *Appl. Opt.*, 21, pp. 3913–18.

LEE, Z. P., CARDER, K. L. and ARNONE, R. A. 2002. Deriving inherent optical properties from water color: a multiband quasi-analytical algorithm for optically deep waters. *Appl. Opt.*, 41, pp. 5755–72.

LEWIS, M. 2007. Measurement of apparent optical properties for diagnosis of harmful algal blooms. In: Babin et al. (eds), op. cit., this volume.

LOISEL, H., BOSC, E., STRAMSKI, D., OUBELKHEIR, K. and DESCHAMPS, P. Y. 2001. Seasonal variability of the backscattering coefficient in the Mediterranean Sea based on satellite SeaWiFS imagery. *Geophys. Res. Lett.*, 28, pp. 4203–06.

LOISEL, H. and MOREL, A. 1998. Light scattering and chlorophyll concentration in Case 1 waters: a reexamination. *Limnol. Oceanogr.*, 43, pp. 847–58.

LOISEL, H., NICOLAS, J. M., DESCHAMPS, P. Y. and FROUIN, R. 2002. Seasonal and inter-annual variability of particulate organic matter in the global ocean. *Geophys. Res. Lett.*, 29, doi:10.1029/2002GL015948.

LOISEL, H. and STRAMSKI, D. 2000. Estimation of the inherent optical properties of natural waters from the irradiance attenuation coefficient and reflectance in the presence of Raman scattering. *Appl. Opt.*, 39, pp. 3001–11.

LUTZ, V. A., SATHYENDRANATH, S. and HEAD, E. J. H. 1996. Absorption coefficient of phytoplankton: regional variations in the North Atlantic. *Mar. Ecol. Progr. Ser.*, 135, pp. 197–213.

MACKEY, M. D., MACKEY, D. J., HIGGINS, H. W. and WRIGHT, S. W. 1996. CHEMTAX – a program for estimating class abundances from chemical markers: application to HPLC measurements of phytoplankton. *Mar. Ecol. Progr. Ser.*, 144, pp. 265–83.

MAFFIONE, R. A. and DANA, D. R. 1997. Instruments and methods for measuring the backward-scattering coefficient of ocean waters. *Appl. Opt.*, 36, pp. 6057–67.

MARITORENA, S., SIEGEL, D. A. and PETERSON, A. R. 2002. Optimization of a semianalytical ocean color model for global-scale application. *Appl. Opt.*, 41, pp. 2705–14.

MILLER, W. L. and ZEPP, R. G. 1995. Photochemical production of dissolved inorganic carbon from terrestrial organic matter: significance to the oceanic organic carbon cycle. *Geophys. Res. Lett.*, 22, pp. 417–20.

MILLIE, D. F., SCHOFIELD, O. M. E., KIRKPATRICK, G. J., JOHNSEN, G. and EVENS, T. J. 2002. Using absorbance and fluorescence spectra to discriminate microalgae. *Eur. J. Phycol.*, 37, pp. 313–22.

MILLIE, D. F., SCHOFIELD, O. M., KIRKPATRICK, G. J., JOHNSEN, G., TESTER, P. A. and VINYARD, B. T. 1997. Detection of harmful algal blooms using photopigments and absorption signatures: a case study of the Florida red tide dinoflagellate, *Gymnodinium breve. Limnol. Oceanogr.*, 2, pp. 1240–51.

MISHONOV, A. V., GARDNER, W. D. and RICHARDSON, M. J. 2003. Remote sensing and surface POC concentration in the South Atlantic. *Deep Sea Res. II*, 50, pp. 2997–3015.

MITCHELL, B. G. and KIEFER, D. A. 1988. Variability in pigment specific particulate fluorescence and absorption spectra in the northeastern Pacific Ocean. *Deep Sea Res.*, 35, pp. 665–89.

MOORE, C. C., TWARDOWSKI, M. S. and ZANEVELD, J. R. V. 2000. The ECO VSF – a sensor for determination of the volume scattering function in the backward direction. *Ocean Optics XV, Proc.* p. 1.

MOORE, C., ZANEVELD, J. R. V. and KITCHEN, J. C. 1992. Preliminary results from an in-situ spectral absorption meter. *Ocean Optics XI, Proc. SPIE*, 1750, pp. 330–37.

MOPPER, K. and KIEBER, D. J. 2002. Photochemistry and the cycling of carbon, sulfur, nitrogen and phosphorus. In: C. A. Carlson (ed.), *Biogeochemistry of Marine Dissolved Organic Matter*. New York, Academic Press, pp. 456–508.

MOREL, A. 1973. Diffusion de la lumière par les eaux de mer. Résultats expérimentaux et approche théorique. In: *Optics of the Sea. AGARD Lect. Ser.*, 61, pp. 3.1.1–3.1.76.

MOREL, A. 1987. Chlorophyll-specific scattering coefficient of phytoplankton. A simplified theoretical approach. *Deep Sea Res.*, 34, pp. 1093–105.

MOREL, A. 1988. Optical modeling of the upper ocean in relation to its biogenous matter content (case I waters). *J. Geophys. Res.*, 93, pp. 10749–68.

MOREL, A. 1997. Consequences of a *Synechococcus* bloom upon the optical properties of oceanic (Case 1) waters. *Limnol. Oceanogr.*, 42(8), pp. 1746–54.

MOREL, A. 2007. Introduction to optical properties in the sea: theoretical aspects. In: Babin et al. (eds), op. cit., this volume.

MOREL, A. AND AHN, Y. H. 1990. Optical efficiency factors of free-living marine bacteria: influence of bacterioplankton upon the optical properties and particulate organic carbon in oceanic waters. *J. Mar. Res.*, 48, pp. 145–75.

MOREL, A. and AHN, Y. H. 1991. Optics of heterotrophic nanoflagellates and ciliates: a tentative assessment of their scattering role in oceanic waters compared to those of bacterial and algal cells. *J. Mar. Res.*, 49, pp. 177–202.

MOREL, A. and BRICAUD, A. 1981*a*. Theoretical results concerning light absorption in a discrete medium, and applications to specific absorption of phytoplankton. *Deep Sea Res.*, 28A, pp. 1375–93.

MOREL, A. and BRICAUD, A. 1981*b*. Theoretical results concerning the optics of phytoplankton, with special reference to remote sensing applications. In: J. F. R. Gower (ed.), *Oceanography from Space*. New York, Plenum Press, pp. 313–27.

MOREL, A. and BRICAUD, A. 1986. Inherent optical properties of algal cells including picoplankton: Theoretical and experimental results. In: T. Platt and W. K. W. Li (eds), *Photosynthetic Picoplankton. Can. Bull. Fish. Aquat. Sci.*, 214, pp. 521–59.

MOREL, A. and GENTILI, B. 1991. Diffuse reflectance of oceanic waters: Its dependence on sun angle as influenced by the molecular scattering contribution. *Appl. Opt.*, 30, pp. 4427–38.

MOREL, A. and MARITORENA, S. 2001. Bio-optical properties of oceanic waters: a reappraisal. *J. Geophys. Res.*, 106, pp. 7163–80.

MOREL, A. and PRIEUR, L. 1977. Analysis of variations in ocean color. *Limnol. Oceanogr.*, 22, pp. 709–22.

NELSON, J. R. and GUARDA, S. 1995. Particulate and dissolved spectral absorption on the continental shelf of the southeastern United States. *J. Geophys. Res.*, 100, pp. 8715–32.

NELSON, N. B. and SIEGEL, D. A. 2002. Chromophoric DOM in the open ocean. In: C. A. Carlson (ed.), *Biogeochemistry of Marine Dissolved Organic Matter*. New York, Academic Press, pp. 547–78.

NELSON, N. B., SIEGEL, D. A. and MICHAELS, A. F. 1998. Seasonal dynamics of colored dissolved material in the Sargasso Sea. *Deep Sea Res. I*, 45, pp. 931–57.

OLSON, R. J., CHISHOLM, S. W., ZETTLER, E. R., ALTABET, M. A. and DUSENBERRY, J. A. 1990. Spatial and temporal distributions of prochlorophyte picoplankton in the North Atlantic Ocean. *Deep Sea Res.*, 37, pp. 1033–51.

OLSON, R. J., SHALAPYONOK, A. A. and SOSIK, H. M. 2003. An automated submersible flow cytometer for pico- and nanophytoplankton: FlowCytobot. *Deep Sea Res. I*, 50, pp. 301–15.

OLSON, R. J., ZETTLER, E. R. and ANDERSON, O. K. 1989. Discrimination of eukaryotic phytoplankton cell types from light scatter and autofluorescence properties measured by flow cytometry. *Cytometry*, 10, pp. 636–43.

OLSON, R. J., ZETTLER, E. R. and DURAND, M. D. 1993. Phytoplankton analysis using flow cytometry. In: P. F. Kemp, B. F. Sherr, E. B. Sherr and J. J. Cole (eds), *Handbook of Methods in Aquatic Microbial Ecology*. Boca Raton, Fla., Lewis Publishers, pp. 175–86.

OPSAHL, S. and BENNER, R. 1997. Distribution and cycling of terrigenous dissolved organic matter in the ocean. *Nature*, 386, pp. 480–82.

O'REILLY, J. E., MARITORENA, S., MITCHELL, B. G., SIEGEL, D. A., CARDER, K. L., GARVER, S. A., KAHRU, M. and McCLAIN, C. R. 1998. Ocean color chlorophyll algorithms for SeaWiFS. *J. Geophys. Res.*, 103, pp. 24937–53.

Pegau, W. S., Deric, G. and Zaneveld, J. R. V. 1997. Absorption and attenuation of visible and near-infrared light in water: dependence on temperature and salinity. *Appl. Opt.*, 36, pp. 6035–46.

Preisendorfer, R. W. 1961. Application of radiative transfer theory to light measurements in the sea. In: *Radiant Energy in the Sea*. Boulder, Colo., International Union of Geodesy and Geophysics, pp. 11–30. (IUGG Monograph 10.)

Preisendorfer, R. W. 1976. *Hydrologic Optics, Volume V. Properties*. Honolulu, Hawaii, US Department of Commerce, National Oceanic and Atmospheric Administration, Environmental Research Laboratories.

Prieur, L. and Sathyendranath, S. 1981. An optical classification of coastal and oceanic waters based on the specific spectral absorption curves of phytoplankton pigments, dissolved organic matter, and other particulate materials. *Limnol. Oceanogr.*, 26, pp. 671–89.

Reckermann, M. and Colijn, F. (eds). 2000. Aquatic flow cytometry: achievements and prospects. *Scientia Marina*, 64(2), pp. 117–268.

Reynolds, R. A., Stramski, D. and Mitchell, B. G. 2001. A chlorophyll-dependent semianalytical reflectance model derived from field measurements of absorption and backscattering coefficients within the Southern Ocean. *J. Geophys. Res.*, 106, pp. 7125–38.

Roesler, C. S. and Boss, E. 2003. Spectral beam attenuation coefficients retrieved from ocean color inversion. *Geophys. Res. Lett.*, 30, 1468, doi:1410.1029/2002GL016185.

Roesler, C. S. and Boss, E. 2007. *In situ* measurement of inherent optical properties and potential for harmful algal bloom detection and coastal ecosystem observations. In: Babin et al. (eds), op. cit., this volume.

Roesler, C. S., Etheridge, S. M. and Pitcher, G. C. 2004. Application of an ocean color algal taxa detection model to red tides in the southern Benguela. In: K. A. Steidinger, J. H. Lansdberg, C. R. Tomas and G. A. Vargo (eds), *Harmful Algae 2002*. Proc. X International Conference on Harmful Algae (20–25 October 2002). St Petersburg, Fla./Paris, Florida Fish and Wildlife Conservation Commission/Intergovernmental Oceanographic Commission of UNESCO, pp. 303–305.

Roesler, C. S., Perry, M. J. and Carder, K. L. 1989. Modeling *in situ* phytoplankton absorption from total absorption spectra in productive inland marine waters. *Limnol. Oceanogr.*, 34, pp. 1510–23.

Roesler, C. S. and Perry, M. J. 1995. *In situ* phytoplankton absorption, fluorescence emission, and particulate backscattering spectra determined from reflectance. *J. Geophys. Res.*, 100, pp. 13279–94.

Ruddick, K., Lacroix, G., Park, Y., Rousseau, V., De Cauwer, V. and Sterckx, S. 2007. Overview of ocean colour: theoretical background, sensors and applicability to detection and monitoring of harmful algal blooms (capabilities and limitations). In: Babin et al. (eds), op. cit., this volume.

Santschi, P. H., Guo, L., Baskaran, K. M., Trumbore, S., Southon, J., Bianchi, T. S., Honeyman, B. and Cifuentes, L. 1995. Isotopic evidence for the contemporary origin of high-molecular weight organic matter in oceanic environments. *Geochim. Cosmochim. Acta*, 59, pp. 625–631.

Sathyendranath, S., Hoge, F. E., Platt, T. and Swift, R. N. 1994. Detection of phytoplankton pigments from ocean color: improved algorithms. *Appl. Opt.*, 33, pp. 1081–89.

Sathyendranath, S., Prieur, L. and Morel, A. 1989. A three-component model of ocean colour and its application to remote sensing of phytoplankton pigments in coastal waters. *Int. J. Rem. Sens.*, 10, pp. 1373–94.

Schofield, O., Bosch, J., Glenn, S., Kirkpatrick, G., Kerfoot, J., Lohrenz, S., Moline, M., Oliver, M. and Bissett, P. 2007. Bio-optics in integrated ocean observing networks: potential for studying harmful algal blooms. In: Babin et al. (eds), op. cit., this volume.

Schofield, O., Grzymski, J., Bissett, W. P., Kirkpatrick, G., Millie, D. F., Moline, M. and Roesler, C. S. 1999. Optical monitoring and forecasting systems for harmful algal blooms: possibility or pipe dream? *J. Phycol.*, 35, pp. 1477–96.

Scholin, C. A., Doucette, G. J. and Cembella, A. D. 2007. Prospects for developing auto-mated systems for *in situ* detection of harmful algae and their toxins. In: Babin et al. (eds), op. cit., this volume.

Siegel, D. A., Dickey, T. D., Washburn, L., Hamilton, M. K. and Mitchell, B. G. 1989. Optical determination of particulate abundance and production variations in the oligotro-phic ocean. *Deep Sea Res.*, 36, pp. 211–22.

Siegel, D. A., Maritorena, S., Nelson, N. B., Hansell, D. A. and Lornenzi-Kayser, M. 2002. Global distribution and dynamics of colored dissolved and detrital organic materials. *J. Geophys. Res.*, 107, 3228, doi:3210.1029/2001JC000965.

Siegel, D. A. and Michaels, A. F. 1996. Quantification of non-algal light attenuation in the Sargasso Sea: implications for biogeochemistry and remote sensing. *Deep Sea Res. II*, 43, pp. 321–45.

Simeon, J., Roesler, C., Pegau, W. S. and Dupouy, C. 2003. Sources of spatial variability in light absorbing components along and equatorial transect from 165°E and 150°W. *J. Geophys. Res.*, 108, 3333, doi:3310.1029/2002JC001613.

Smith, R. C. and Baker, K. S. 1978. Optical classification of natural waters. *Limnol. Oceanogr.*, 23, pp. 260–67.

Smyth, T. J., Moore, G. F., Groom, S. B., Land, P. E. and Tyrell, T. 2002. Optical modeling and measurements of a coccolithophore bloom. *Appl. Opt.*, 41, pp. 7679–88.

SooHoo, J. B., Kiefer, D. A., Collins, D. J. and McDermid, I. S. 1986. *In vivo* fluorescence excitation and absorption spectra of marine phytoplankton. I: Taxonomic characteristics and responses to photoadaptation. *J. Plankton Res.*, 8, pp. 197–214.

Sosik, H. M., Green, R. E., Pegau, W. S. and Roesler, C. S. 2001. Temporal and vertical vari-ability in optical properties of New England shelf waters during late summer and spring. *J. Geophys. Res.*, 106, pp. 9455–72.

Sosik, H. M. and Mitchell, B. G. 1991. Absorption, fluorescence and quantum yield for growth in nitrogen limited *Dunaliella tertiolecta. Limnol. Oceanogr.*, 36, pp. 910–21.

Sosik, H. M. and Mitchell, B. G. 1995. Light absorption by phytoplankton, photosynthetic pigments, and detritus in the California Current System. *Deep Sea Res.*, 42, pp. 1717–48.

Sosik, H. M., Olson, R. J., Neubert, M. G., Shalapyonok, A. A. and Solow, A. R. 2003. Growth rates of coastal phytoplankton from time-series measurements with a submersible flow cytometer. *Limnol. Oceanogr.*, 48, pp. 1756–65.

Sosik, H. M., Vernet, M. and Mitchell, B. G. 1992. A comparison of particulate absorption properties between high- and mid-latitude surface waters. *Antarct. J. Unit. States*, 27, pp. 162–64.

Stramska, M., Stramski, D., Mitchell, B. G. and Mobley, C. D. 2000. Estimation of the absorption and backscattering coefficients from in-water radiometric measurements. *Lim-nol. Oceanogr.*, 45, pp. 628–41.

Stramski, D., Bricaud, A. and Morel, A. 2001. Modeling the inherent optical properties of the ocean based on the detailed composition of the planktonic community. *Appl. Opt.*, 40, pp. 2929–45.

Stramski, D. and Kiefer, D. A. 1991. Light scattering by microorganisms in the open ocean. *Progr. Oceanogr.*, 28, pp. 343–83.

Stramski, D. and Morel, A. 1990. Optical properties of photosynthetic picoplankton in differ-ent physiological states as affected by growth irradiance. *Deep Sea Res.*, 37, pp. 45–266.

Stramski, D., Reynolds, R. A., Kahru, M. and Mitchell, B. G. 1999. Estimation of particu-late organic carbon in the ocean from satellite remote sensing. *Science*, 285, pp. 239–42.

Stramski, D., Wozniak, S. B. and Flatau, P. J. 2004. Optical properties of Asian mineral dust suspended in seawater. *Limnol. Oceanogr.*, 49, pp. 749–55.

Stumpf, R. P. 2001. Application of satellite ocean color sensors for monitoring and predicting harmful algal blooms. *Hum. Ecol. Risk Assess.*, 7, pp. 1363–68.

Subramaniam, A., Brown, C. W., Hood, R. R., Carpenter, E. J. and Capone, D. G. 2002. Detecting *Trichodesmium* blooms in SeaWiFS imagery. *Deep Sea Res. II*, 49, pp. 107–21.

SUBRAMANIAM, A. and CARPENTER, E. J. 1994. An empirically derived protocol for the detection of blooms of the marine cyanobacterium *Trichodesmium* using CZCS imagery. *Int. J. Rem. Sens.*, 15, pp. 1559–69.

SUBRAMANIAM, A., CARPENTER, E. J. and FALKOWSKI, P. G. 1999. Bio-optical properties of the marine diazotrophic cyanobacteria *Trichodesmium* spp. II: A reflectance model for remote sensing. *Limnol. Oceanogr.*, 44, pp. 618–27.

TWARDOWSKI, M. S., BOSS, E., MACDONALD, J. B., PEGAU, W. S., BARNARD, A. H. and ZANEVELD, J. R. V. 2001. A model for estimating bulk refractive index from the optical backscattering ratio and the implications for understanding particle composition in case I and case II waters. *J. Geophys. Res.*, 106, pp. 14129–42.

TWARDOWSKI, M. S., BOSS, E., SULLIVAN, J. M. and DONAGHAY, P. L. 2004. Modeling the spectral shape of absorption by chromophoric dissolved organic matter. *Mar. Chem.*, 89, pp. 69–88.

TWARDOWSKI, M. S. and DONAGHAY, P. L. 2001. Separating *in situ* and terrigenous sources of absorption by dissolved materials in coastal waters. *J. Geophys. Res.*, 106, pp. 2545–60.

TWARDOWSKI, M. S. and DONAGHAY, P. L. 2002. Photobleaching of aquatic dissolved materials: absorption removal, spectral alteration, and their interrelationship. *J. Geophys. Res.*, 107, doi:10.1029/1999JC000281.

TYRELL, T., HOLLIGAN, P. M. and MOBLEY, C. D. 1999. Optical impacts of oceanic coccolithophore blooms. *J. Geophys. Res.*, 104, pp. 3223–41.

ULLOA, O., SATHYENDRANATH, S. and PLATT, T. 1994. Effect of the particle-size distribution on the backscattering ratio in seawater. *Appl. Opt.*, 33, pp. 7070–77.

VODACEK, A., BLOUGH, N. V., DEGRANDPRE, M. D., PELTZER, E. T. and NELSON, R. K. 1997. Seasonal variation of CDOM and DOC in the Middle Atlantic Bight: terrestrial inputs and photooxidation. *Limnol. Oceanogr.*, 42(4), pp. 674–86.

VODACEK, A., HOGE, F. E., SWIFT, D. G., KUNGEL, J. K., PELTZER, E. T. and BLOUGH, N. V. 1995. The use of *in situ* and airborne fluorescence measurements to determine UV absorption coefficients and DOC concentrations in surface waters. *Limnol. Oceanogr.*, 40, pp. 411–15.

VOSS, K. J. 1992. A spectral model of the beam attenuation coefficient in the ocean and coastal areas. *Limnol. Oceanogr.*, 37, pp. 501–09.

VOSS, K. J., BALCH, W. M. and KIRKPATRICK, K. A. 1998. Scattering and attenuation properties of *Emiliania huxleyi* cell and their detached coccoliths. *Limnol. Oceanogr.*, 43, pp. 870–76.

YENTSCH, C. S. 1960. The influence of phytoplankton pigments on the colour of sea water. *Limnol. Oceanogr.*, 7, pp. 1–9.

YENTSCH, C. S. 1962. Measurement of visible light absorption by particulate matter in the ocean. *Limnol. Oceanogr.*, 7, pp. 207–17.

YENTSCH, C. S. and MENZEL, D. W. 1963. A method for the determination of phytoplankton and phaeophytin by fluorescence. *Deep Sea Res.*, 10, pp. 221–31.

YENTSCH, C. S. and PHINNEY, D. A. 1985. Spectral fluorescence: an ataxonomic tool for studying the structure of phytoplankton populations. *J. Plankton Res.*, 7, pp. 617–32.

YENTSCH, C. S. and PHINNEY, D. A. 1989. A bridge between ocean optics and microbial ecology. *Limnol. Oceanogr.*, 34, pp. 1694–1705.

ZANEVELD, J. R. V. 1974. New developments of the theory of radiative transfer in the oceans. In: N. G. Jerlov and E. S. Nielsen (eds), *Optical Aspects of Oceanography*. New York, Academic Press, pp. 121–34.

ZANEVELD, J. R. V. and KITCHEN, J. C. 1995. The variation in the inherent optical properties of phytoplankton near an absorption peak as determined by various models of cell structure. *J. Geophys. Res.*, 100, pp. 13309–20.

ZANEVELD, J. R. V., ROACH, D. R. and PAK, H. 1974. The determination of the index of refraction distribution of oceanic particulates. *J. Geophys. Res.*, 79, pp. 4091–95.

ZANEVELD, J. R. V., TWARDOWSKI, M. S., SHIFRIN, K. S., PEGAU, W. S., BOSS, E. and ZOLOTOV, I. 2002. Inversion of light scattering measurements to obtain biogeochemical parameters. *Ocean Optics XVI, Proc.* pp. 1–19.